RESEARCH

A CMIP6 multi-model ensemble-based analysis of potential climate change impacts on irrigation water demand and supply using SWAT and CROPWAT models: a case study of Akmese Dam, Turkey

Emrah Yalcin[1]

Abstract

This study details an integrated framework for assessing the water supply reliability of a multi-purpose reservoir under different climate change scenarios, with the case of the Akmese Project in northwest Turkey. In this assessment, the precipitation and temperature simulations of 24 Global Circulation Models (GCMs) from the Couple Model Intercomparison Project phase 6 (CMIP6) are analyzed using two statistical bias correction methods, namely, linear scaling and distribution mapping, to produce the best-performing multi-model ensemble predictions under two different Shared Socio-economic Pathway (SSP) scenarios (SSP245 and SSP585). The future inflow rates of the Akmese reservoir are simulated using the Soil and Water Assessment Tool (SWAT) model. The CROPWAT model is utilized to estimate crop water and crop irrigation requirements under the projected climate conditions. The effects of changing climate on the lake evaporation rates are also taken into consideration in analyzing the future reservoir water availability for domestic usages, irrigation demands, and downstream environmental flow requirements. The 25-year monthly reservoir operations are conducted with the changing inputs of the projected inflows, lake evaporation rates, and irrigation requirements for the historical period of 1990–2014 and near-, mid-, and long-future periods of 2025–2049, 2050–2074, and 2075–2099, respectively. The results indicate that the projected changes in the hydro-climatic conditions of the Akmese Basin will adversely impact the reservoir water availability. Under the high-forcing scenario SSP585, 9.26 and 22.11% of the total water demand, and 20.17 and 38.89% of the total irrigation requirement cannot be supplied, in turn, in the mid- and long-future periods.

Keywords CMIP6 · Multi-model ensemble · SWAT model · Irrigation · Water availability · Mediterranean

1 Introduction

Water scarcity is a severe problem in the Mediterranean region (10° W, 40° E, 30° N, 45° N; Iturbide et al. 2020), with predominantly arid and semi-arid climate conditions (Iglesias et al. 2007; UNDP 2006; Yang and Zehnder 2002). In most countries of the region, water resources management and allocation practices have been challenging due to the strong climate seasonality characterized by mild and wet winters, during which most of the precipitation and runoff events occur, and hot and dry summers with little precipitation (Bolle 2003; Kondolf and Batalla 2005; Milano et al.

2013; Montaldo and Oren 2018). The demand for irrigation water increases during the summer months as the growing season progresses. Variations in the availability and demand for water result in temporary or permanent water scarcity (Gorguner and Kavvas 2020). Seasonal and inter-annual water storage reservoirs regulating natural river flows have been a common remedy for the Mediterranean countries to meet their growing water demands resulting from population growth, expansion of irrigated agriculture, and increasing industrial and tourism activities (Choukr-Allah et al. 2012; Correia 1999; Cudennec et al. 2007; Kondolf and Batalla 2005; UNDP 2006). Irrigated agriculture is the largest consumer of freshwater from these reservoirs and accounts for 21% of the total cultivated agricultural land in the region (Daccache et al. 2014).

In addition to the current challenges, future climate change is expected to pose a significant threat to the water resources of the Mediterranean region. According

✉ Emrah Yalcin
emrah.yalcin@ahievran.edu.tr

1 Department of Civil Engineering, Kirsehir Ahi Evran University, 40100 Kirsehir, Turkey

to Giorgi (2006), the Mediterranean region is one of the most vulnerable zones in the world to both climatic and anthropogenic changes, making it a climate change hot-spot. All climate change assessments for the Mediterranean Basin and its sub-regions indicate ongoing warming of the atmosphere and the sea, as well as projected higher temperatures and changes in rainfall (Ali et al. 2022; Cherif et al. 2020; Stocker et al. 2013). Besides the projected warming climate, the main risk factors are drought and irrigation water scarcity expected to increase generally over the region (Hoegh-Guldberg et al. 2022; Jiménez Cisneros et al. 2014; Kovats et al. 2014; Mrabet et al. 2020). These projections have led to growing concern about declines in water storage due to the combined effects of future precipitation and temperature regime changes on the water balance components of reservoirs, such as river runoff, water demands, and lake evaporation (Braca et al. 2019; Koutroulis et al. 2016; Masia et al. 2018; Okkan and Kirdemir 2018; Tramblay et al. 2020). However, modeling the hydro-climatic impacts of the Mediterranean region is a very challenging task due to the high spatial and temporal variability of its climate characterized by a complicated morphology (Gorguner and Kavvas 2020; Lionello et al. 2006; Michaelides et al. 2018; Şen 2015). Therefore, to adequately assess the regional and local-scale impacts, high spatial resolution and quality in climate information are required (Zittis et al. 2022).

Despite many previous studies examining the potential impacts of future climate change on the climate and hydrology of the Mediterranean basins, a few researchers have extended their analyses to evaluate the effects of these changes on the operational efficiency and long-term sustainability of agricultural reservoirs. For instance, Haro-Monteagudo et al. (2020) assessed the effects of climate change on the hydrology and water management in the Gállego-Cinca River System of the Ebro Basin of Spain using the ensemble projections of 22 statistically downscaled General Circulation Models (GCMs) from the Couple Model Intercomparison Project phase 5 (CMIP5) under moderate and high Representative Concentration Pathway (RCP) scenarios, namely, RCP4.5 and RCP8.5, respectively. Another example is the study by Gorguner and Kavvas (2020), who used a dynamic water balance model with the climate projections of the dynamically downscaled outputs of four CMIP5 GCMs to assess how climate change could affect the water balance of an agricultural reservoir in the Gediz Basin of Turkey under the RCP4.5 and RCP8.5 scenarios. López-Moreno et al. (2014), Nunes et al. (2017), Okkan and Kirdemir (2018), Rocha et al. (2020), and Valverde et al. (2015) are some other examples that have analyzed the future changes in reservoir inflows, storage capacity, and irrigation water requirements in different basins of the Mediterranean using GCM projections from the CMIP3 and CMIP5 databases (i.e., the third and fifth phases of CMIP, respectively).

The latest release of CMIP, the sixth phase (CMIP6), features several improvements compared to its predecessors, CMIP3 and CMIP5. These improvements focus mainly on quantifying the radiative forcing arising from natural phenomena and human activities, including greenhouse gas concentrations, representation of aerosol forcing, and changes in land use (Eyring et al. 2016; Stouffer et al. 2017; Wyser et al. 2020). CMIP6 projections are based on alternative scenarios of future emissions and land use changes released under new features of societal development, namely, the Shared Socioeconomic Pathways (SSPs). SSPs are not only an updated version of their counterparts in CMIP5 (i.e., RCPs) but also incorporate current emission trends (O'Neill et al. 2016). While there is no distinguishable change in the overall projections between the CMIP3 and CMIP5 ensembles (Knutti and Sedláček 2013; Kumar et al. 2014), several CMIP6 models project greater global warming than the previous generation of models throughout the twenty-first century (Forster et al. 2020). Cos et al. (2022) analyzed the Mediterranean climate change based on the CMIP5 and CMIP6 ensemble projections. According to their findings, the projected warming during the summer season ranges from 1.83 to 8.49 °C in CMIP6 and 1.22 to 6.63 °C in CMIP5 by the end of the century, considering three different scenarios and 50% of the inter-model spread. In contrast to temperature, the projected precipitation changes showed higher uncertainty and spatial heterogeneity. However, under the high emission scenario, a substantial decline in precipitation was projected over large parts of the region during the summer months (from -49 to -16% in CMIP6 and from -47 to -22% in CMIP5). According to Bağçaci et al. (2021), who compared the temperature and precipitation projections of the ensembles of the best-performing GCMs from the CMIP5 and CMIP6 databases over Turkey, CMIP6 products outperform CMIP5 in terms of accuracy metrics, particularly for precipitation. The study also reports that the projected changes in climate across the country are summer warming (up to 6.5 °C) and drying (up to 40%) towards the autumn months. Despite these changes in the climate projections, to the best of the knowledge, there is no study in the literature investigating the effects of climate change on the future sustainability of irrigation reservoirs in the Mediterranean region under the CMIP6 climate scenarios.

The main objective of this study is to quantify the potential impacts of future climate change on irrigation demands and the water balance of a multi-purpose reservoir, considering the statistically downscaled precipitation and temperature simulations of 24 GCMs from the CMIP6 archive under the medium- and high-forcing SSP scenarios, namely, SSP245 and SSP585, respectively. The Akmese Dam and Irrigation Project in northwest Turkey is chosen as the study

case. The project's feasibility and environmental impact assessment were examined using the historical hydro-meteorological data in 2016, and the construction works have not yet started (Temelsu 2016a, b). The Akmese reservoir is planned to provide domestic, irrigation, and environmental water requirements in a water-scarce basin representing the typical hydro-climatic conditions of the eastern Mediterranean region. The assessment relies on the climate projections of the best-performing multi-model ensembles generated by analyzing the outputs of the 24 CMIP6 GCMs using two different bias correction methods, namely, linear scaling and distribution mapping. The monthly inflow rates of the Akmese reservoir are simulated through the calibrated and validated Soil and Water Assessment Tool (SWAT) model of the dam basin using the daily climate projections of the best-performing multi-model ensembles under the CMIP6 historical experiment and future scenarios of SSP245 and SSP585 (O'Neill et al. 2016). The CROPWAT model is preferred to estimate crop water and crop irrigation requirements under the projected climate conditions. The projected changes in the net evaporation rates of the Akmese reservoir are also taken into consideration in analyzing the future reservoir water availability. The reservoir operations are performed on a monthly basis using the estimated inflow, irrigation requirements, and net evaporation rates for the historical and near-, mid-, and long-future periods. The projected impacts of climate change on water availability, spillway releases, and regulation ratio are evaluated in 25-year periods by considering the operation results obtained under the climate conditions of the CMIP6 historical experiment as the baseline scenario. This study is expected to provide insight into the urgent need for adaptation strategies in the ongoing planning and operation practices for coping with the increasing risks of water scarcity across the Mediterranean basins.

2 Study area and hydro-climatological data

The Akmese Project lies between the latitudes 40°40′ and 41°10′ N, and the longitudes 29°55′ and 30°30′ E within the borders of Kocaeli Province in the Marmara Region of Turkey, as presented in Fig. 1. The Akmese Dam is planned on Budaklar Creek which is a branch of the Sakarya River discharging into the Black Sea. In the current situation, during the period from May to September when irrigation is intense in the region, the flows of Budaklar Creek decrease considerably, and irrigation water demand is not met. In addition, the amount of domestic water supplied from Sapanca Lake
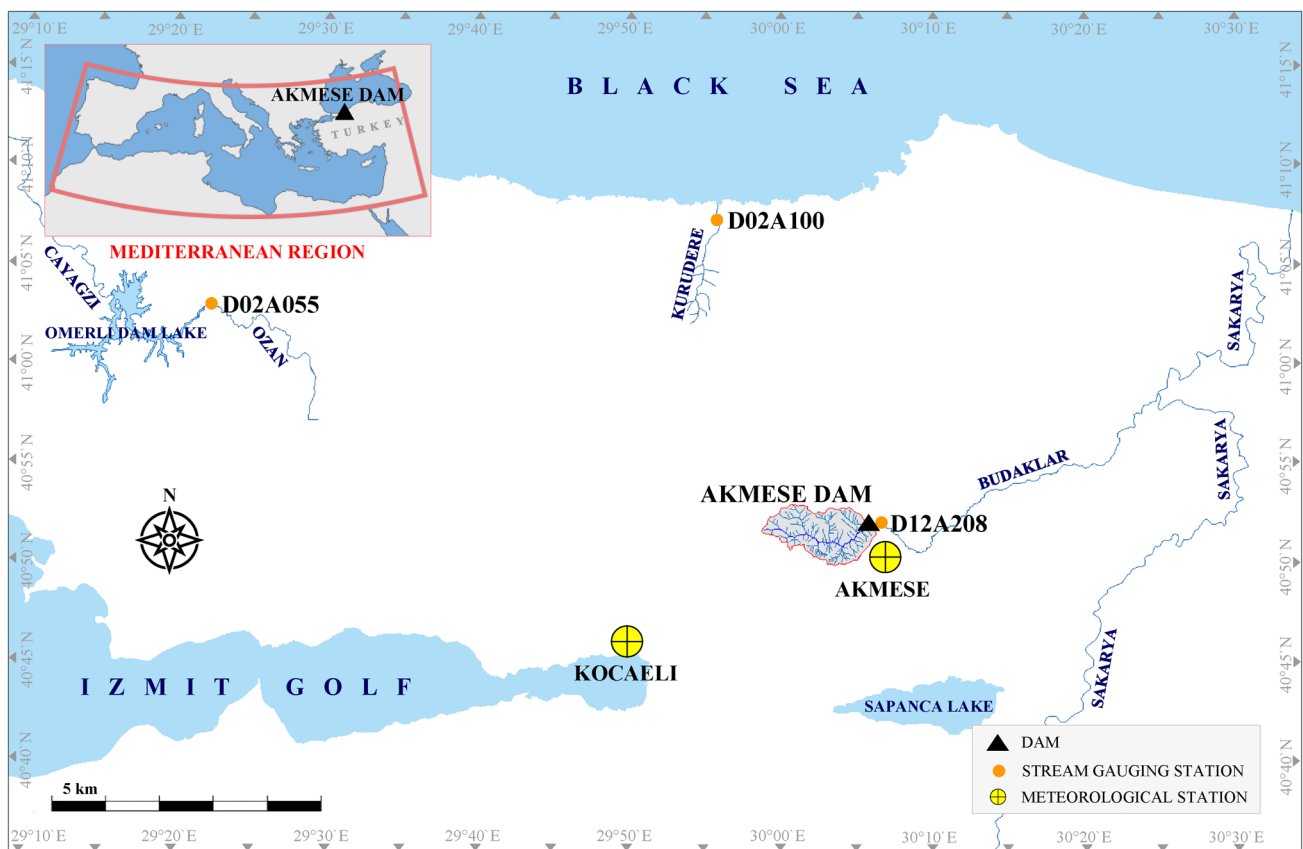

Fig. 1 Location map of the study area and hydro-meteorological stations

and its sources needs to be reduced since the lake basin, one of the most important wetlands of the country, is under the threat of drought. The purpose of the project is to supply water for irrigation and domestic use needs with an active reservoir volume of 13.58 hm³. It is planned to irrigate a gross area of 1742 ha, of which the net irrigation area is 1521 ha, through gravity and pumped pipeline systems. The proposed crop pattern in this area to be irrigated composes of cereals (25%), fruits (18%), legumes (12%), maize (10%), tomato (10%), pepper (10%), potato (8%), and alfalfa (7%), with cabbage (3%) and other vegetables (3%) as the secondary products. A volume of 7.19 hm³ is to be provided annually for domestic usage from the dam reservoir to the municipal water system of Kocaeli Province. Moreover, an annual volume of 2.83 hm³ is planned to be left on the riverbed as environmental water for the maintenance of the natural ecosystem (Temelsu 2016a, b).

The flows of Budaklar Creek, draining an area of 36.9 km² from its source to the Akmese Dam location, are measured at the Akmese stream-gauging station (SGS) (Station ID: D12A208) (Fig. 1). The Akmese station, operated by the General Directorate of State Hydraulic Works (DSI), has a drainage area of 40.6 km², and its intermittent flow records are not sufficient alone to be utilized in the hydrological model calibration and validation processes (DSI 2022). Due to the absence of flow measurements from the Budaklar Basin to extend the records of the Akmese SGS, the flow records of the DSI's Bickidere (Station ID: D02A055) and Pargali (Station ID: D02A100) stations, which have a drainage area of 87 and 37 km², respectively, are utilized to constitute reasonably long and continuous historical inflow time series for the Akmese reservoir (Fig. 1) (DSI 2022). By using the strong correlation relationships between the monthly mean flow measurements of the Akmese station and these two representative stations of the neighboring basins, a 25-year monthly flow dataset of the 1990–2014 period is produced for the Akmese station. The 211 months of this 300-month dataset consist of raw data from the Akmese station, and the missing data for 89 months are completed using the correlations having Pearson's r values above 0.80. Accordingly, while the mean flow rate for the records at the Akmese station in 1990–2014 is 0.50 m³/s, the mean of the extended flow dataset is determined to be 0.52 m³/s. The extended flow records of the Akmese station are brought to the dam location based on the catchment area ratio between the Akmese station and Akmese Dam. Accordingly, the mean historical inflow rate of the Akmese Dam is determined as 0.47 m³/s or 14.92 hm³/year.

The climatic variables required for the hydrological model, crop irrigation requirement, and lake evaporation analyses to be conducted in the historical flow period of 1990–2014 are precipitation, maximum and minimum temperatures, wind speed, relative humidity, solar radiation, insolation, and evaporation. The nearest representative meteorological station (MS) that has the long-term measurements of all these variables is the Kocaeli station (Station ID: 17066), operated by the Turkish State Meteorological Service (MGM) at an altitude of 74 m (Fig. 1). According to the long-term weather records of the Kocaeli MS (i.e., in 1949–2021), the mean annual temperature is 15 °C, and the annual total precipitation average is 821 mm (MGM 2022c). Although the closest station to the Akmese Basin is the Akmese MS of MGM (Station IDs: 1532 and 18799), this station was operated in the 1984–1993 period and became operational again in 2017 (Fig. 1). At the same time, solar radiation, insolation, and evaporation measurements are not performed at this station (MGM 2022b). In this study, all climatic analyses of the Akmese Basin and Akmese irrigation scheme are based on the measurements of the Kocaeli MS.

3 Applied methodology

In this study, climate change impacts on the net water requirements of the Akmese irrigation scheme and the reservoir storage sufficiency of the Akmese Dam for meeting water demands are assessed in 25-year periods from the historical 1990–2014 period to the near-, mid-, and long-future periods of 2025–2049, 2050–2074, and 2075–2099, respectively. The framework of this assessment consists of six main stages: (1) producing daily predictions of maximum and minimum temperature and precipitation for the location of the Kocaeli MS under the CMIP6 historical experiment and future scenarios of SSP245 and SSP585, (2) development of a SWAT model for the Akmese Basin using the daily weather records of the Kocaeli MS, (3) calibration and validation of the SWAT model using the monthly streamflow records at the dam location and estimation of the monthly streamflow rates for the historical and future periods, (4) estimation of the mean monthly net irrigation requirements of the Akmese irrigation scheme for the historical and future periods, (5) estimation of the mean monthly lake evaporation rates for the historical and future periods, and (6) performing reservoir operations for the historical and future periods and examination of the vulnerabilities of the Akmese Project to future climate conditions. The flowchart of the applied methodology is depicted in Fig. 2.

3.1 Generating climate change scenarios using the multi-model ensembles of CMIP6 GCMs

In this study, the daily precipitation, maximum temperature, and minimum temperature simulations of the 24 CMIP6 GCMs, obtained from the Earth System Grid Federation (ESGF) website (ESGF 2022), are considered to produce the multi-model ensemble mean predictions for the coordinates
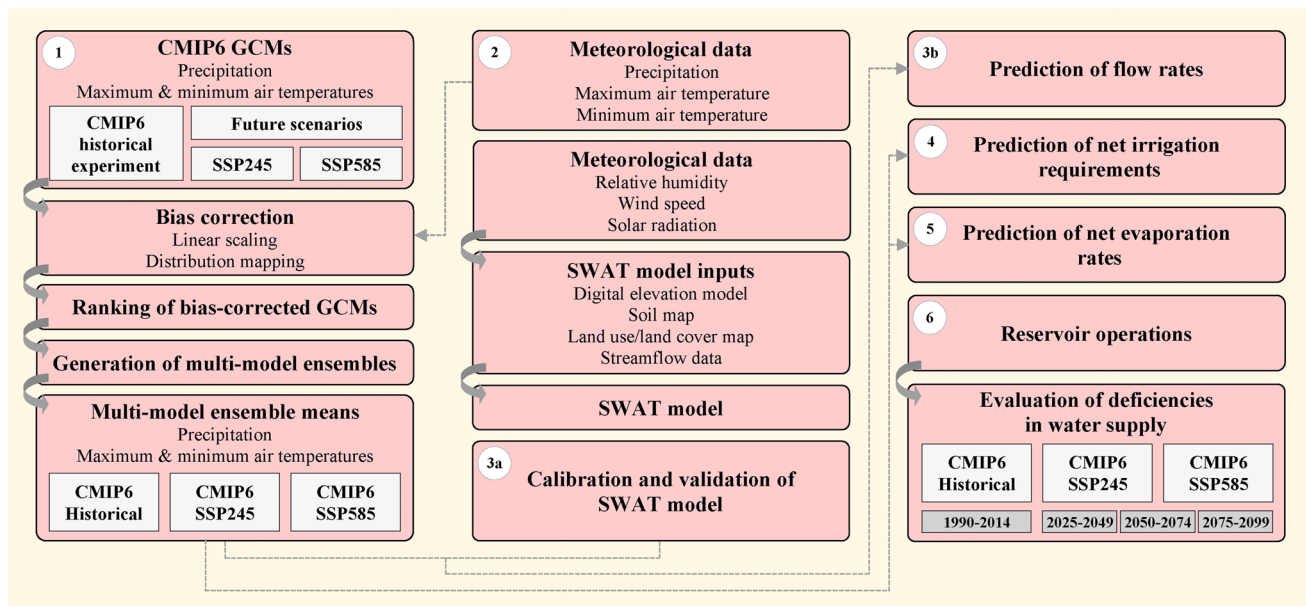
Fig. 2 Schematic illustration of the applied methodology

of the Kocaeli MS under the CMIP6 historical experiment and future emission scenarios of SSP245 and SSP585. The details of these GCMs are listed in Table 1. In order to provide consistency and perform fair comparisons, the GCM selection is based on the availability of daily simulations under the first ensemble member (i.e., with a variant label of r1i1p1f1) (Sun et al. 2022), and the datasets of the selected GCMs are uniformly interpolated to a spatial resolution of $0.5° \times 0.5°$ using the first-order conservative remapping method (Jones 1999). The aggregation, manipulation, and interpolation operations of the GCM datasets are performed within the Cygwin terminal (Cygwin 2022) using the Climate Data Operators (CDO) software (Schulzweida 2021).

Two statistical bias correction methods, linear scaling and distribution mapping, are employed separately to adjust the GCM simulations against possible systematic errors for the location of the Kocaeli MS. The bias corrections are performed within the Climate Model Data for Hydrologic Modelling (CMhyd) tool (Rathjens et al. 2016) by using the daily measurements of the Kocaeli MS (MGM 2022a) between 1950 and 2014, which is the common period with the CMIP6 historical experiment simulations. Modified index of agreement (*md*) (Legates and McCabe 1999), normalized root mean square error (nRMSE) (Almeida et al. 2015), Kling-Gupta efficiency metric (KGE) (Gupta et al. 2009), and fractions skill score (FSS) (Roberts and Lean 2008) are considered as the performance measures in evaluating the performances of the bias-corrected historical simulations of the GCMs on a monthly basis. For each bias correction method, the GCMs are ranked from best to worst for each climate variable separately according to their

comprehensive rating metric (RM) (Chen et al. 2011) computed by considering all four performance measures. For the temperature variables, an overall ranking of the GCMs is derived by combining the comprehensive RMs obtained for the maximum and minimum temperature variables.

There is no well-defined guideline in the literature on selecting the optimum number of GCMs in generating a multi-model ensemble to reduce uncertainties in climate projections; nevertheless, the use of the top-ranked 3 to 10 GCMs is widespread (Ahmed et al. 2019; Bağçaci et al. 2021). In this study, the top-four ranked GCMs are considered to generate multi-model ensembles for each climate variable. The daily time series of the multi-model ensembles under the CMIP6 historical experiment and future emission scenarios of SSP245 and SSP585 are produced according to the simple mean technique by just averaging the daily bias-corrected simulations of the top-four ranked GCMs (Ahmed et al. 2019). The performance measures of the multi-model ensemble means observed under the use of the linear scaling and distribution mapping methods are compared separately for each climate variable. Accordingly, the best-performing multi-model ensemble means are determined to be used in assessing the hydrological changes related to these climate variables in the Akmese Basin.

The historical analysis period of this study is determined to be 1990–2014, depending on the available inflow data of the Akmese reservoir. Hence, the precipitation and temperature predictions of the best-performing multi-model ensembles under the CMIP6 historical experiment in this period are regarded as the baseline climate scenario. All the changes in inflow rates, lake evaporations, and irrigation water demands

Table 1 List of the CMIP6 GCMs selected for climate model evaluation

Model ID	Institution	Resolution in arc degrees	
		(latitude)	(longitude)
ACCESS-CM2	Commonwealth Scientific and Industrial Research Organization (CSIRO), Australia Australian Research Council Centre of Excellence for Climate System Science (ARC-CSS), Australia	1.25	1.875
ACCESS-ESM1-5	Commonwealth Scientific and Industrial Research Organization (CSIRO), Australia	1.25	1.875
BCC-CSM2-MR	Beijing Climate Center (BCC), China	1.112–1.121	1.125
CanESM5	Canadian Centre for Climate Modelling and Analysis (CCCma), Canada	2.767–2.791	2.8125
CMCC-ESM2	Centro Euro-Mediterraneo sui Cambiamenti Climatici (CMCC), Italy	0.9424084	1.25
EC-Earth3	EC-Earth Consortium, Europe	0.696–0.702	0.703125
EC-Earth3-CC	EC-Earth Consortium, Europe	0.696–0.702	0.703125
EC-Earth3-Veg	EC-Earth Consortium, Europe	0.696–0.702	0.703125
EC-Earth3-Veg-LR	EC-Earth Consortium, Europe	1.112–1.121	1.125
FGOALS-g3	Chinese Academy of Sciences (CAS), China	2.025–5.181	2
GFDL-CM4	National Oceanic and Atmospheric Administration-Geophysical Fluid Dynamics Laboratory (NOAA-GFDL), USA	1	1.25
GFDL-ESM4	National Oceanic and Atmospheric Administration-Geophysical Fluid Dynamics Laboratory (NOAA-GFDL), USA	1	1.25
INM-CM4-8	Institute for Numerical Mathematics (INM), Russia	1.5	2
INM-CM5-0	Institute for Numerical Mathematics (INM), Russia	1.5	2
IPSL-CM6A-LR	Institut Pierre Simon Laplace (IPSL), France	1.267606	2.5
KIOST-ESM	Korea Institute of Ocean Science and Technology (KIOST), Korea	*for precipitation data* 1.875 *for temperature data* 1.894737	1.875
MIROC6	Japan Agency for Marine-Earth Science and Technology (JAMSTEC), Japan Atmosphere and Ocean Research Institute-The University of Tokyo (AORI), Japan National Institute for Environmental Studies (NIES), Japan RIKEN Center for Computational Science (R-CCS), Japan	1.389–1.401	1.40625
MPI-ESM1-2-HR	Max Planck Institute for Meteorology (MPI-M), Germany Deutsches Klimarechenzentrum (DKRZ), Germany	0.927–0.935	0.9375
MPI-ESM1-2-LR	Max Planck Institute for Meteorology (MPI-M), Germany	1.850–1.865	1.875
MRI-ESM2-0	Meteorological Research Institute (MRI), Japan	1.112–1.121	1.125
NESM3	Nanjing University of Information Science and Technology (NUIST), China	1.850–1.865	1.875
NorESM2-LM	NorESM Climate Modeling Consortium, Norway	1.894737	2.5
NorESM2-MM	NorESM Climate Modeling Consortium, Norway	0.9424084	1.25
TaiESM1	Research Center for Environmental Changes-Academia Sinica (AS-RCEC), Taiwan	0.9424084	1.25

are evaluated using the best-performing multi-model mean predictions in the 2025–2049, 2050–2074, and 2075–2099 periods under the future scenarios of SSP245 and SSP585. For convenience, the best-performing multi-model ensemble mean predictions under the CMIP6 historical experiment and future emission scenarios of SSP245 and SSP585 are also referred to as the CMIP6 Historical, CMIP6 SSP245, and CMIP6 SSP585, respectively, in the rest of text.

3.2 Setting up the SWAT model

SWAT is a physically based hydrological model developed by the United States Department of Agriculture-Agricultural Research Service (USDA-ARS) (Arnold et al. 2013; Neitsch

et al. 2011). In this study, the SWAT model is constructed within ArcSWAT 2012 (revision 664) using the coarse-scale geospatial data of the Akmese Basin and the daily weather records of the Kocaeli MS to simulate the inflow rates of the Akmese reservoir on a monthly basis under potential climate change conditions. The geospatial data utilized in the model setup include (1) void-filled digital elevation model (DEM) obtained from the Shuttle Radar Topography Mission (SRTM) database at approximately 30 m resolution (USGS 2014), (2) land cover map extracted from the Global Land Cover 2000 (GLC2000) version 2.0 dataset at 1 km spatial resolution (EC-JRC 2006), and (3) soil map derived from the Digital Soil Map of the World (DSMW) version 3.6 dataset at a scale of 1:5 million (FAO 2007). SWAT

divides the delineated watershed of the Akmese Dam into 109 subbasins considering the inputted DEM data. These subbasins are further subdivided into a total of 443 hydrologic response units (HRUs) having unique combinations of land cover, soil, and topographic slope characteristics. The topographic, land cover, soil, and slope characteristics of the Akmese Basin are presented in Fig. 3. The daily precipitation, maximum and minimum air temperature, solar radiation, wind speed, and relative humidity observations of the Kocaeli MS between 1986 and 2014, including four years of warm-up period (i.e., 1986–1989), are inputted into the developed model together with the long-term mean monthly weather statistics of the station (i.e., in 1949–2021) (MGM 2022a). The built-in weather generator of SWAT uses these statistics in producing representative daily values not only for the few-day gaps in the observed data but also for the unavailable solar radiation, relative humidity, and wind speed predictions under the CMIP6 historical experiment and future scenarios of SSP245 and SSP585.

3.3 Calibration and validation of the SWAT model and flow simulations under changing climate

The developed SWAT model is calibrated and validated against the historical flow rates at the Akmese Dam location on a monthly basis. The runoff data in the first 17 years of the historical analysis period (i.e., 1990–2006) is used to calibrate the model for monthly flow simulations, and the validation of the calibrated model is conducted against the runoff data of the remaining 8 years (i.e., 2007–2014). The sensitivity, calibration, validation, and uncertainty analyses of the developed SWAT model are performed within the SWAT Calibration and Uncertainty Procedures (SWAT-CUP) software package (Abbaspour 2015). The Sequential Uncertainty Fitting Version 2 (SUFI-2) algorithm (Abbaspour et al. 2004, 2007) is preferred as the optimization procedure to estimate the best ranges of the sensitive modeling parameters. Nash–Sutcliffe Efficiency (NSE) (Nash and Sutcliffe 1970) is utilized as the objective function of the SUFI-2 algorithm.

In the calibration process, the sensitivity of each modeling parameter is evaluated separately through a single iteration with 50 simulations. After identifying sensitive parameters and their initial ranges in these one-at-a-time analyses, combined iterations composed of 500 simulations are repeated by narrowing the initial parameter ranges at each time until (1) most of the observed flow data is bracketed by the 95% prediction uncertainty (95PPU) band, and (2) average width of the 95PPU band is smaller than the standard deviation of the observed flows. The strength of the calibration is evaluated by these two indices, known as the P factor and R factor, respectively (Abbaspour et al. 2004). Accordingly, the final iteration, where acceptable values of P factor and R factor are reached, has the best ranges for the parameters in concern, and the best simulation of the final iteration with the highest objective function value provides the best-performing parameter set (Abbaspour et al. 2015). After terminating the model calibration for the 1990–2006
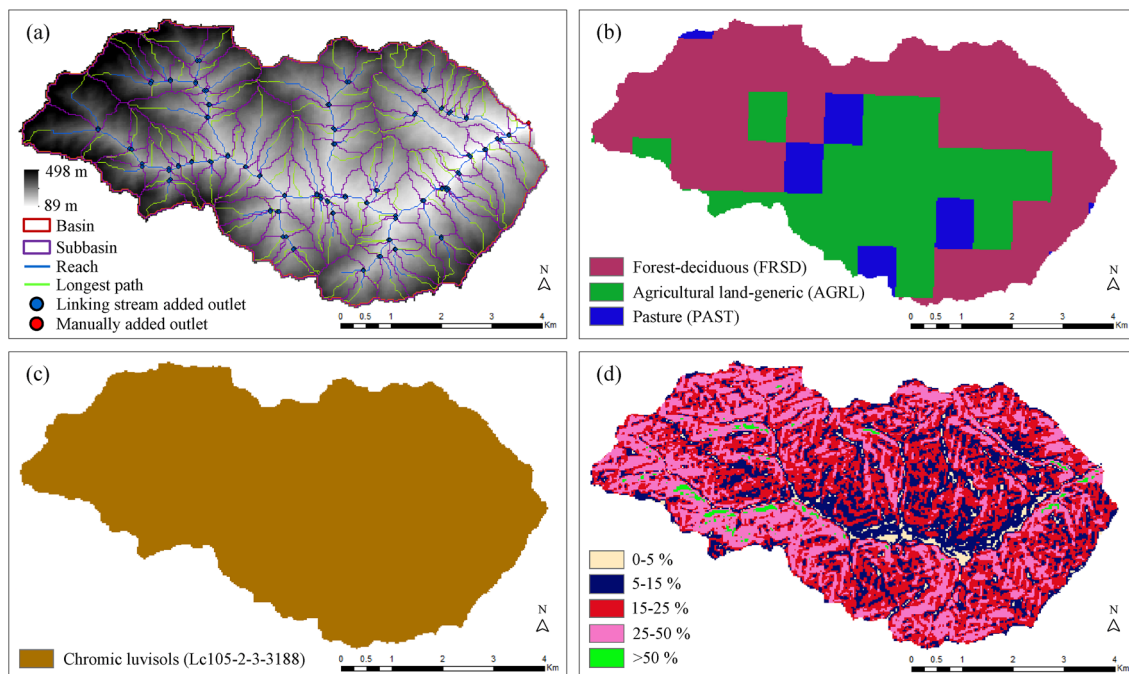

Fig. 3 Steps of the SWAT model setup: **a** DEM and watershed delineation, **b** land cover classes, **c** soil types, and **d** slope classes

period, the calibrated model performance is validated against the monthly inflow rates of the Akmese reservoir in 2007–2014 by performing a single combined iteration composed of 500 simulations within the calibrated parameter ranges.

In addition to the objective function NSE, the calibrated and validated model performances in terms of the best simulation are evaluated by the statistics of percent bias (PBIAS) and the ratio of the root mean square error to the standard deviation of observed flows (RSR). However, all these statistics obtained for the best simulation results do not reflect the flow forecasting performance of the SWAT model in the absence of flow records because the best simulation results attained in the model calibration and validation stages belong to the simulation with the highest NSE value against the historical flow data. Hence, the usability of the best-performing parameter set of the calibration period is verified by performing a single simulation for the validation period (Yalcin 2019). The results of this simulation, referred to as the best simulation estimates, are evaluated again in terms of the statistics of NSE, PBIAS, and RSR. After verifying the flow forecasting performance of the SWAT model, the model simulations under the use of the best-performing parameter set of the calibration are performed for the historical and near-, mid-, and long-future periods by introducing the precipitation and temperature predictions of the CMIP6 Historical, CMIP6 SSP245, and CMIP6 SSP585.

3.4 Irrigation water demand under changing climate

The effects of climate change on the water requirements of the crops to be grown within the Akmese irrigation district are investigated using the CROPWAT 8.0 software developed by the Land and Water Development Division of the Food and Agricultural Organization of the United Nations (FAO) (Smith 1992). CROPWAT is designed to calculate reference evapotranspiration (ET_o) and to simulate crop water requirements (ET_c) and irrigation demands based on the inputted climate, soil, and crop data. CROPWAT utilizes the FAO Penman–Monteith method (Allen et al. 1998) to compute the mean daily ET_o rates per month by considering the mean monthly statistics of maximum and minimum temperatures, relative humidity, wind speed, and daily sunshine hours. The United States Department of Agriculture Soil Conservation Service (USDA SC) methodology (USDA-SCS 1970) is selected to obtain the mean monthly total effective rainfall amounts based on the given average total precipitation data per month.

Before introducing the mean monthly maximum and minimum temperature statistics to the CROPWAT model, the temperature predictions of the CMIP6 Historical, CMIP6 SSP245, and CMIP6 SSP585 for the historical and near-,

mid-, and long-future periods are transformed into the mean elevation of the Akmese irrigation area (i.e., around 100 m), assuming a 1 °C decrease in temperature per 200 m increase in altitude. For the other climate data to estimate the ET_o rates, the mean monthly long-term statistics of the Kocaeli MS records between 1949 and 2021 are used for the considered historical and future time periods (MGM 2022c). The effective rainfall estimates of the CROPWAT model under the analyzed climate scenarios are based on the inputted mean monthly statistics of the precipitation predictions obtained for the Kocaeli MS location. Considering the extracted soil characteristics of the Akmese irrigation area from DSMW version 3.6 (FAO 2007), the clay loam soil texture of the region is evaluated to be the heavy type among the specified FAO soil classes within the software (Allen et al. 1998; Ansley et al. 2014).

The crop pattern of the irrigation scheme proposed in Temelsu (2016a) is identified according to the areal coverage of each crop. CROPWAT calculates the ET_c amounts by multiplying ET_o and appropriate crop coefficients (K_c). The crop characteristics related to the planting and harvest dates, days of the growth stages (initial, development, mid-season, and late-season), and K_c values (for the initial stage, mid-season stage, and at harvest) are taken from the report analyzing the water requirements of irrigated crops on station basis for the climatic regions of Turkey (TAGEM and DSI 2017). The other crop data on rooting depth, critical depletion, and yield response factor are based on the characteristics of the related FAO crops specified within the software (Allen et al. 1998).

The irrigation schedules are developed under the introduced climate conditions with the selected options of irrigating at a fixed interval of 10 days per stage and refilling soil moisture content to the field capacity. In addition, the farm and irrigation efficiencies are set to 0.90 and 0.98, respectively, considering the piped conveyance system and irrigation methods (i.e., sprinkler and drip) to be applied in the irrigation scheme (Temelsu 2016a). CROPWAT determines the irrigation water requirements of the project crops using the estimated ET_c and effective rainfall amounts. Accordingly, under an overall irrigation efficiency of 0.88, the mean monthly net irrigation water requirements of the Akmese irrigation scheme are calculated separately for the historical and three future time periods by running the CROPWAT model with the given precipitation and transformed temperature predictions of the considered climate scenarios.

3.5 Evaporation from the Akmese reservoir under changing climate

The long-term correlation relationship between the mean monthly total evaporation and temperature records of the Kocaeli MS for the 1949–2021 period is used to estimate the

mean monthly net evaporation rates of the Akmese reservoir under the CMIP6 historical experiment and future scenarios of SSP245 and SSP585 (MGM 2022c). The arithmetic mean of the daily maximum and minimum temperature predictions is taken as the daily mean temperature, and accordingly, calculated mean monthly temperature predictions for the location of the Kocaeli MS are transformed into the maximum water level of the Akmese reservoir (i.e., 137.7 m) under the assumption that temperature decreases by 1 °C for every 200 m rise in altitude. The monthly actual evaporation rates from the Akmese reservoir surface are calculated by multiplying the monthly evaporations corresponding to the transformed monthly lake surface temperatures in the correlation relationship with the pan correction coefficient of 0.7 (Usul 2009). The mean monthly net evaporation estimates per unit area are computed by subtracting the mean monthly precipitation predictions from the calculated monthly actual evaporation rates. This procedure is repeated for the historical and near-, mid-, and long-future periods by using the precipitation and temperature predictions of the CMIP6 Historical, CMIP6 SSP245, and CMIP6 SSP585.

3.6 Multi-purpose reservoir operation algorithm

The operation studies of the Akmese reservoir are conducted on a monthly basis through a multi-purpose operation algorithm written in Visual Basic for Applications in Excel software. The operation algorithm is prepared based on the physical and operational characteristics of the project specified in the feasibility and environmental impact assessment reports (Temelsu 2016a, b). The physical reservoir characteristics are described through the use of the volume-area and elevation curves. The operational data include the maximum and minimum operation levels, spillway capacity, and mean monthly domestic and environmental water demands. The maximum and minimum water levels of the reservoir are 137.7 m and 112.5 m, respectively. The spillway capacity of the Akmese Dam is designated to be 243 m³/s. While the domestic water supply is targeted to be a total of 7.19 hm³ per year, with amounts ranging from 0.48 to 0.75 hm³ per month, the minimum amounts of environmental water to be released downstream for the continuation of natural life are determined as 0.154, 0.135, 0.112, 0.123, and 0.063 m³/s for January, February, March and April, December, and the remaining months, respectively (Temelsu 2016a, b). Besides, these fixed inputs of the operation algorithm, the reservoir inflow rates, lake evaporation rates, and irrigation water demands estimated under the considered climate scenarios are the changing inputs of the reservoir operations. For all reservoir operations, the initial reservoir volume is set to be equal to the maximum storage capacity. In case the amount of storage is lower than the monthly total water demand, the priority order of water supply is constrained

to be domestic, environmental, and irrigation. Accordingly, the operation studies are repeated for the historical and near, mid-, and long-future periods under the climate conditions of the CMIP6 historical experiment and future scenarios of SSP245 and SSP585 to assess climate change impacts on water supply security for the Akmese Project.

4 Results and discussions

4.1 Climate change scenarios

The statistical performances of the bias-corrected monthly precipitation, maximum temperature, and minimum temperature prediction time series of the 24 GCMs under the CMIP6 historical experiment against the measurements of the Kocaeli MS in the 1950–2014 period are given in Table 2 and Table 3 for the cases of using linear scaling and distribution mapping, respectively. While the values nearest to 1 refer to the best model performance in terms of the *md*, KGE, and FSS statistics, the GCMs are ranked starting from the best model having the closest value to 0 regarding the nRMSE metric. The ranking of the GCMs for the precipitation variable is based on the RM values, and the RM value nearest to 1 refers to the best model performance for the precipitation predictions. For the maximum and minimum temperature variables, the overall ranking of the GCMs is determined by considering the overall RM values based on the individual RM rankings of the GCMs obtained for each temperature variable. According to the attained GCM rankings, indicated in bold text in Table 2 and Table 3, the top-four ranked GCMs are selected as the members of the multi-model ensembles for the precipitation and temperature predictions at the Kocaeli MS location.

The comparisons of the statistical performance metrics of the multi-model ensemble means show that the best-performing bias correction method is linear scaling for both precipitation and temperature variables, as detailed in Table 4. Accordingly, the members of the multi-model ensembles are GFDL-ESM4, MRI-ESM2-0, ACCESS-ESM1-5, and GFDL-CM4 for the precipitation variable and BCC-CSM2-MR, MIROC6, CMCC-ESM2, and MRI-ESM2-0 for the maximum and minimum temperature variables. Although the statistical performances of the multi-model ensemble means are higher than the individual performance metrics of all the 24 GCMs for each climate variable, the monthly precipitation predictions cannot be improved significantly even with the use of the multi-model ensemble, as in the cases of Ahmed et al. (2019), Bağçaci et al. (2021), Seker and Gumus (2022), and Siqueira et al. (2021). Nevertheless, the mean monthly, seasonal, and annual precipitation predictions of the multi-model ensemble have close agreements with the mean precipitation records of the Kocaeli MS. While the

Table 2 Performance metrics and ranks of GCMs after bias correction using the linear scaling method. Bold numbers within brackets indicate the rank of GCMs

GCM	Precipitation					Minimum temperature					Maximum temperature					Temperature
	md	nRMSE	KGE	FSS	RM (rank)	md	nRMSE	KGE	FSS	RM	md	nRMSE	KGE	FSS	RM	RM (rank)
ACCESS-CM2	0.403	0.194	0.192	0.734	0.375 (**16**)	0.810	0.112	0.906	0.989	0.083	0.812	0.108	0.899	0.978	0.073	0.083 (**22**)
ACCESS-ESM1-5	0.422	0.179	0.259	0.772	0.833 (**3**)	0.802	0.119	0.894	0.987	0.000	0.810	0.110	0.896	0.978	0.021	0.000 (**24**)
BCC-CSM2-MR	0.401	0.187	0.186	0.746	0.417 (**14**)	0.871	0.075	0.951	0.995	0.948	0.879	0.066	0.958	0.992	0.958	0.958 (**1**)
CanESM5	0.428	0.185	0.259	0.755	0.792 (**5**)	0.846	0.090	0.941	0.993	0.510	0.846	0.088	0.936	0.986	0.271	0.375 (**15**)
CMCC-ESM2	0.388	0.198	0.179	0.724	0.198 (**20**)	0.852	0.085	0.944	0.993	0.740	0.864	0.074	0.952	0.990	0.875	0.792 (**3**)
EC-Earth3	0.403	0.197	0.189	0.730	0.302 (**18**)	0.835	0.096	0.932	0.992	0.240	0.829	0.098	0.920	0.982	0.125	0.188 (**20**)
EC-Earth3-CC	0.429	0.204	0.206	0.717	0.448 (**11**)	0.846	0.091	0.939	0.993	0.438	0.846	0.087	0.937	0.986	0.292	0.354 (**16**)
EC-Earth3-Veg	0.407	0.211	0.168	0.702	0.188 (**21**)	0.836	0.096	0.931	0.992	0.219	0.831	0.095	0.925	0.984	0.198	0.208 (**19**)
EC-Earth3-Veg-LR	0.416	0.191	0.219	0.741	0.615 (**7**)	0.824	0.105	0.919	0.990	0.167	0.832	0.096	0.923	0.983	0.177	0.167 (**21**)
FGOALS-g3	0.389	0.187	0.194	0.749	0.438 (**13**)	0.817	0.111	0.907	0.989	0.125	0.813	0.110	0.891	0.978	0.031	0.083 (**23**)
GFDL-CM4	0.416	0.175	0.236	0.776	0.802 (**4**)	0.849	0.087	0.943	0.993	0.625	0.846	0.083	0.942	0.987	0.438	0.521 (**12**)
GFDL-ESM4	0.434	0.175	0.267	0.778	0.958 (**1**)	0.842	0.092	0.935	0.992	0.333	0.855	0.083	0.942	0.987	0.448	0.396 (**13**)
INM-CM4-8	0.415	0.192	0.224	0.742	0.604 (**8**)	0.845	0.088	0.942	0.993	0.552	0.850	0.081	0.945	0.988	0.552	0.583 (**9**)
INM-CM5-0	0.406	0.189	0.245	0.750	0.604 (**9**)	0.843	0.091	0.938	0.993	0.375	0.844	0.086	0.938	0.986	0.313	0.354 (**17**)
IPSL-CM6A-LR	0.408	0.195	0.213	0.737	0.479 (**10**)	0.837	0.095	0.933	0.992	0.292	0.848	0.085	0.940	0.987	0.385	0.333 (**18**)
KIOST-ESM	0.411	0.176	0.252	0.773	0.760 (**6**)	0.803	0.117	0.899	0.988	0.042	0.860	0.078	0.949	0.989	0.729	0.396 (**14**)
MIROC6	0.403	0.196	0.196	0.735	0.375 (**17**)	0.867	0.078	0.952	0.995	0.927	0.871	0.072	0.957	0.990	0.917	0.917 (**2**)
MPI-ESM1-2-HR	0.407	0.202	0.214	0.726	0.385 (**15**)	0.847	0.088	0.942	0.993	0.552	0.864	0.076	0.952	0.989	0.833	0.688 (**7**)
MPI-ESM1-2-LR	0.420	0.205	0.218	0.719	0.448 (**12**)	0.850	0.087	0.943	0.993	0.667	0.853	0.082	0.944	0.988	0.500	0.583 (**10**)
MRI-ESM2-0	0.430	0.181	0.261	0.766	0.854 (**2**)	0.856	0.086	0.944	0.993	0.750	0.862	0.076	0.951	0.989	0.792	0.771 (**4**)
NESM3	0.414	0.215	0.197	0.702	0.281 (**19**)	0.861	0.083	0.944	0.994	0.844	0.859	0.080	0.946	0.988	0.646	0.750 (**5**)
NorESM2-LM	0.400	0.238	0.086	0.648	0.031 (**24**)	0.853	0.085	0.945	0.993	0.781	0.856	0.078	0.950	0.989	0.708	0.750 (**6**)
NorESM2-MM	0.412	0.213	0.168	0.699	0.177 (**22**)	0.856	0.085	0.946	0.994	0.844	0.855	0.081	0.945	0.988	0.552	0.688 (**8**)
TaiESM1	0.394	0.209	0.176	0.705	0.135 (**23**)	0.845	0.091	0.939	0.993	0.448	0.857	0.080	0.947	0.988	0.667	0.563 (**11**)

Table 3 Performance metrics and ranks of GCMs after bias correction using the distribution mapping method. Bold numbers within brackets indicate the rank of GCMs

GCM	Precipitation					Minimum temperature					Maximum temperature					Temperature
	md	nRMSE	KGE	FSS	RM (rank)	md	nRMSE	KGE	FSS	RM	md	nRMSE	KGE	FSS	RM	RM (rank)
ACCESS-CM2	0.385	0.223	0.119	0.674	0.104 (**21**)	0.823	0.105	0.919	0.990	0.104	0.835	0.094	0.926	0.983	0.000	0.042 (**23**)
ACCESS-ESM1-5	0.400	0.214	0.193	0.706	0.667 (**7**)	0.819	0.109	0.912	0.989	0.042	0.836	0.094	0.926	0.984	0.042	0.042 (**24**)
BCC-CSM2-MR	0.374	0.223	0.118	0.678	0.094 (**24**)	0.832	0.100	0.926	0.991	0.396	0.849	0.083	0.942	0.987	0.448	0.417 (**14**)
CanESM5	0.401	0.220	0.167	0.688	0.333 (**18**)	0.832	0.098	0.929	0.991	0.573	0.855	0.082	0.944	0.987	0.729	0.625 (**8**)
CMCC-ESM2	0.379	0.210	0.158	0.700	0.417 (**14**)	0.834	0.097	0.931	0.992	0.823	0.853	0.081	0.945	0.988	0.813	0.896 (**2**)
EC-Earth3	0.397	0.207	0.180	0.711	0.740 (**4**)	0.829	0.100	0.926	0.991	0.406	0.850	0.085	0.940	0.987	0.406	0.417 (**15**)
EC-Earth3-CC	0.426	0.208	0.206	0.710	0.917 (**1**)	0.837	0.097	0.931	0.992	0.792	0.855	0.082	0.944	0.988	0.792	0.833 (**3**)
EC-Earth3-Veg	0.398	0.215	0.164	0.693	0.385 (**15**)	0.827	0.102	0.922	0.991	0.292	0.842	0.088	0.934	0.986	0.125	0.208 (**19**)
EC-Earth3-Veg-LR	0.402	0.211	0.187	0.705	0.688 (**6**)	0.826	0.105	0.919	0.990	0.188	0.844	0.089	0.935	0.986	0.115	0.146 (**20**)
FGOALS-g3	0.370	0.222	0.128	0.683	0.125 (**20**)	0.836	0.098	0.929	0.991	0.646	0.854	0.083	0.943	0.987	0.604	0.604 (**10**)
GFDL-CM4	0.385	0.217	0.167	0.700	0.365 (**17**)	0.829	0.099	0.927	0.991	0.458	0.847	0.082	0.943	0.987	0.521	0.479 (**12**)
GFDL-ESM4	0.409	0.214	0.204	0.706	0.729 (**5**)	0.823	0.104	0.920	0.990	0.188	0.852	0.085	0.940	0.987	0.385	0.250 (**18**)
INM-CM4-8	0.409	0.216	0.174	0.695	0.510 (**12**)	0.833	0.097	0.931	0.992	0.771	0.853	0.081	0.945	0.988	0.792	0.771 (**4**)
INM-CM5-0	0.394	0.220	0.175	0.693	0.375 (**16**)	0.831	0.101	0.925	0.991	0.354	0.849	0.085	0.940	0.987	0.406	0.354 (**16**)
IPSL-CM6A-LR	0.403	0.212	0.182	0.704	0.635 (**9**)	0.822	0.105	0.919	0.990	0.115	0.843	0.088	0.936	0.986	0.135	0.146 (**21**)
KIOST-ESM	0.390	0.220	0.171	0.690	0.281 (**19**)	0.812	0.112	0.908	0.989	0.000	0.846	0.087	0.938	0.986	0.229	0.104 (**22**)
MIROC6	0.388	0.210	0.171	0.705	0.542 (**11**)	0.842	0.094	0.935	0.992	0.927	0.852	0.082	0.943	0.988	0.646	0.771 (**5**)
MPI-ESM1-2-HR	0.404	0.211	0.195	0.707	0.760 (**3**)	0.838	0.094	0.935	0.992	0.938	0.862	0.076	0.951	0.989	0.958	0.958 (**1**)
MPI-ESM1-2-LR	0.410	0.217	0.187	0.697	0.573 (**10**)	0.826	0.103	0.922	0.991	0.240	0.845	0.086	0.939	0.986	0.271	0.271 (**17**)
MRI-ESM2-0	0.412	0.208	0.208	0.714	0.917 (**2**)	0.839	0.097	0.930	0.991	0.792	0.854	0.081	0.944	0.988	0.771	0.771 (**6**)
NESM3	0.397	0.243	0.101	0.650	0.104 (**22**)	0.832	0.100	0.926	0.991	0.479	0.853	0.083	0.942	0.987	0.542	0.521 (**11**)
NorESM2-LM	0.392	0.231	0.109	0.660	0.104 (**23**)	0.833	0.098	0.929	0.991	0.667	0.851	0.081	0.945	0.988	0.813	0.771 (**7**)
NorESM2-MM	0.414	0.211	0.179	0.700	0.656 (**8**)	0.837	0.098	0.929	0.991	0.729	0.847	0.086	0.937	0.986	0.260	0.479 (**13**)
TaiESM1	0.393	0.210	0.168	0.697	0.479 (**13**)	0.834	0.099	0.928	0.991	0.583	0.854	0.082	0.944	0.987	0.698	0.625 (**9**)

Table 4 Performance metrics of the multi-model ensemble means obtained using the linear scaling and distribution mapping methods. Statistics for the averages of raw climate data (without any correction) from the member GCMs are presented within brackets

Climate variable	Bias correction method	Member GCMs	md	nRMSE	KGE	FSS
Precipitation	Linear scaling	GFDL-ESM4 MRI-ESM2-0 ACCESS-ESM1-5 GFDL-CM4	0.445 (0.432)	0.145 (0.154)	0.271 (0.230)	0.836 (0.820)
	Distribution mapping	EC-Earth3-CC MRI-ESM2-0 MPI-ESM1-2-HR EC-Earth3	0.442 (0.420)	0.156 (0.164)	0.272 (0.211)	0.814 (0.784)
Maximum temperature	Linear scaling	BCC-CSM2-MR MIROC6 CMCC-ESM2 MRI-ESM2-0	0.879 (0.807)	0.070 (0.103)	0.954 (0.892)	0.996 (0.990)
	Distribution mapping	MPI-ESM1-2-HR CMCC-ESM2 EC-Earth3-CC INM-CM4-8	0.871 (0.865)	0.074 (0.080)	0.951 (0.904)	0.995 (0.994)
Minimum temperature	Linear scaling	BCC-CSM2-MR MIROC6 CMCC-ESM2 MRI-ESM2-0	0.892 (0.712)	0.060 (0.138)	0.962 (0.619)	0.993 (0.971)
	Distribution mapping	MPI-ESM1-2-HR CMCC-ESM2 EC-Earth3-CC INM-CM4-8	0.887 (0.881)	0.063 (0.065)	0.958 (0.939)	0.993 (0.992)

mean annual total precipitation, maximum temperature, and minimum temperature rates of the Kocaeli MS records in the historical analysis period of 1990–2014 are 831.28 mm, 20.09 °C, and 11.23 °C, these means are determined to be 825.06 mm, 20.22 °C, and 11.38 °C for the CMIP6 Historical predictions, respectively.

Considering the climate predictions attained under the CMIP6 historical experiment as the baseline scenario, the future changes in the climate between 2025 and 2099 under the emission scenarios of SSP245 and SSP585 are analyzed in 25-year periods, as summarized in Table 7. Accordingly, under the SSP245 scenario, although the differences in the mean annual total precipitation between the historical period and three future periods are less than 4%, the mean summer total precipitation amounts are 11.59, 20.85, and 24.91% less than the mean of the CMIP6 Historical predictions for the near-, mid-, and long-future periods, respectively. In addition, the decrease in the mean autumn total precipitation is projected to be 6.71% over the long-future period. The mean annual maximum and minimum temperatures are projected to increase gradually through the future periods, and these increases reach 2.59

and 2.49 °C, respectively, in the 2075–2099 period. Under the SSP585 scenario, while the mean annual total precipitation amounts decrease, in turn, by 6.14 and 7.68% in the near- and mid-future periods, there is a sharp decrease of 15.47% over the long-future period. The mean summer total precipitation amounts decrease by 25.38, 33.30, and 55.23% in the near, mid-, and long-future periods, respectively. The decreases in the mean autumn total precipitation are determined, in turn, to be 10.98 and 19.35% for the mid- and long-future periods. The projected gradual increases in the mean annual maximum and minimum temperatures under the SSP585 emission scenario reach 4.20 and 3.82 °C in the 2075–2099 period, respectively. Bağçaci et al. (2021) analyzed the precipitation and temperature changes for the 2030–2050, 2050–2070, and 2070–2100 periods over the seven geographical regions of Turkey using the ensemble projections of the best-performing GCMs from the CMIP6 database. It is seen that the attained precipitation and temperature anomalies for the coordinates of the Kocaeli station in this study are highly consistent with their results for the Marmara Region, which covers the Kocaeli station location.

4.2 SWAT model performance and changing climate impacts on reservoir inflows

The developed SWAT model is calibrated by adjusting the parameter ranges of 14 sensitive modeling parameters related to the groundwater, soil, management, HRU, and main channel input files. These parameters are listed starting from the most sensitive one with their calibrated ranges and best-performing values in Table 5. Figure 4a shows the monthly time series of the simulated and observed streamflow rates at the Akmese Dam location for the 1990–2006 period. The last combined iteration performed with the calibrated parameter ranges provides a satisfactory 95PPU band with the *P* and *R* factor values of 0.82 and 0.78, respectively. Abbaspour et al. (2015) suggest a *P* factor value greater than 0.70 and an *R* factor value less than 1.50 in establishing the balance between these two factors for monthly streamflow simulations. The objective function NSE, PBIAS, and RSR statistics of the best simulation of this combined iteration are determined, in turn, to be 0.77, 9.08%, and 0.48, as detailed in Table 6. According to the performance classification of Moriasi et al. (2007) regarding monthly streamflow simulations, the calibrated model performance in terms of the best simulation is categorized as very good with the attained NSE value of more than 0.75, PBIAS value of less than $\pm 10\%$, and RSR value of less than 0.50.

The monthly simulation outputs for the validation period of 2007–2014 are presented in Fig. 4b, and the statistical performance metrics are provided in Table 6. As in the case of the calibration, a reasonable 95PPU band with a *P* factor value of 0.83 and an *R* factor value of 0.92 is obtained for the

validation period. While the performance of the best simulation is similar to the one of the calibration in terms of the NSE and RSR metrics, a much less PBIAS value of -3.18% is attained for the validation period. Hence, the model performance is also classified as very good for the validation period (Moriasi et al. 2007). Regarding the forecasting ability of the SWAT model, the best simulation estimates show a similar performance with the best simulation of the validation in terms of all the considered statistics, as presented in Fig. 4b and detailed in Table 6.

After verifying the usability of the best-performing parameter set of the calibration for the validation period, the model is run with the precipitation and temperature predictions under the CMIP6 historical experiment and future emission scenarios of SSP585 and SSP585 to forecast the inflow rates of the Akmese reservoir in the historical and near-, mid-, and long-future periods. The resultant monthly flow forecasts simulated through these model runs are summarized with their seasonal and annual averages in Table 7. Accordingly, while the mean inflow rates of the Akmese reservoir based on the SGS records are 0.27, 0.91, 0.55, 0.16, and 0.47 m^3/s during autumn, winter, spring, summer, and annually in the historical analysis period of 1990–2014, the SWAT model simulation with the CMIP6 Historical predictions results in the inflow rates of 0.25, 1.08, 0.50, 0.17, and 0.50 m^3/s, respectively. Considering the streamflow estimates attained under the CMIP6 historical experiment as the baseline scenario, the projected changes in the streamflow rates at the Akmese Dam location are evaluated in three 25-year future periods on a seasonal and annual basis (Table 7).

Table 5 List of the calibrated parameters

Sensitive modeling parameter[a]	Calibrated parameter range	Best-performing parameter value
Baseflow alpha factor (1/days), v__ALPHA_BF.gw	[0.1, 1]	0.133
Effective hydraulic conductivity in main channel alluvium (mm/hr), v__CH_K2.rte	[100, 500]	196.4
Depth from soil surface to bottom of layer (mm), r__SOL_Z().sol	[−0.7, 2.33]	0.067
Initial SCS runoff curve number for moisture condition II, r__CN2.mgt	[−0.2, 0.1]	0.082
Plant uptake compensation factor, v__EPCO.hru	[0, 1]	0.711
Soil evaporation compensation factor, v__ESCO.hru	[0, 1]	0.815
Deep aquifer percolation fraction, v__RCHRG_DP.gw	[0, 1]	0.823
Groundwater *revap* coefficient, v__GW_REVAP.gw	[0.02, 0.2]	0.139
Maximum canopy storage (mm H_2O), v__CANMX.hru	[0, 100]	59.7
Saturated hydraulic conductivity (mm/hr), r__SOL_K().sol	[−0.99, 262.157]	86.638
Groundwater delay time (days), v__GW_DELAY.gw	[0, 500]	407.5
Moist bulk density (mg/m^3 or g/cm^3), r__SOL_BD().sol	[−0.307, 0.666]	0.085
Threshold depth of water in the shallow aquifer required for return flow to occur (mm H_2O), v__GWQMN.gw	[0, 5000]	935
Available water capacity of the soil layer (mm H_2O/ mm soil), v__SOL_AWC().sol	[0.1, 1]	0.317

[a]The qualifier v__ refers to the substitution of a parameter by a value from the given range, and r__ refers to a relative change in the parameter for which the current value is multiplied by 1 plus a factor in the given range
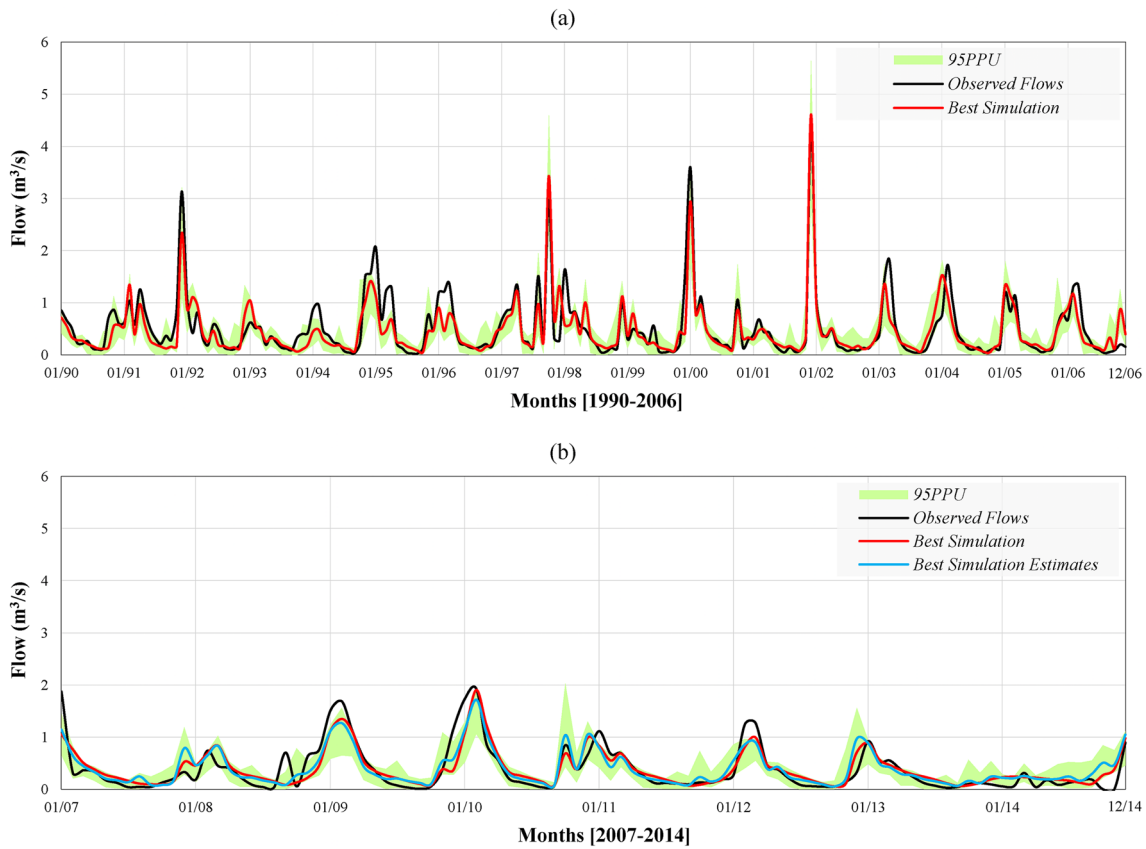
Fig. 4 Simulation outputs of the SWAT model at the Akmese Dam location for the **a** calibration and **b** validation periods

Table 6 Statistical performance indices for the calibration and validation periods

Model simulation	NSE	PBIAS (%)	RSR	Mean (m³/s)		Standard deviation (m³/s)	
				Simulation	Observed	Simulation	Observed
Calibration period (1990–2006)							
Best simulation	0.77	9.08	0.48	0.47	0.52	0.54	0.60
Validation period (2007–2014)							
Best simulation	0.76	− 3.18	0.49	0.40	0.38	0.34	0.44
Best simulation estimates	0.74	− 4.61	0.51	0.40		0.34	

Under the SSP245 emission scenario, while the mean annual inflow rates of the Akmese reservoir reduce gradually by 4.66, 5.81, and 8.05% in the 2025–2049, 2050–2074, and 2075–2099 periods, respectively, the inflow reductions in the autumn months of the 2050–2074 and 2075–2099 periods are markedly higher than the annual inflow decreases. The decreases in the mean flow rate of the autumn months are 10.17 and 17.84% in the mid- and long-future periods, respectively. Under the SSP585 emission scenario, the inflow declines are much more pronounced than under the SSP245 scenario. The mean annual inflow rates are 10.00, 13.59, and 26.17% less than the annual mean of the historical period for the near-,

mid-, and long-future periods, respectively. While the mean inflow decreases in the winter and summer seasons are similar to the annual reductions as in the case under the SSP245 scenario, the means of the autumn months are 22.93, 33.23, and 59.15% less than the historical autumn average in the 2025–2049, 2050–2074, and 2075–2099 periods, respectively. For the spring season, while the mean inflow reduction is projected to be 20.05% in the long-future period, the decrease percentages are only 3.17 and 1.97% for the near- and mid-future periods, respectively. For both emission scenarios, the significant reductions in the autumn flows show the effect of the projected severe summer and autumn precipitation decreases on the

Table 7 Seasonal and annual comparisons of the total precipitation and maximum and minimum temperature predictions for the Kocaeli MS location, streamflow estimates for the Akmese Dam location, total net evaporation rates of the Akmese reservoir, and total net irrigation requirements of the Akmese irrigation scheme obtained under the CMIP6 historical experiment and future emission scenarios of SSP245 and SSP585

Climate data		CMIP6 Historical	CMIP6 SSP245			CMIP6 SSP585		
Analysis period		1990–2014	2025–2049	2050–2074	2075–2099	2025–2049	2050–2074	2075–2099
Total precipitation (mm)	Autumn	228.39	222.02	219.47	213.06	216.26	203.32	184.20
	Winter	286.65	290.48	290.26	296.74	283.27	288.90	286.97
	Spring	174.64	171.28	179.36	181.06	173.81	179.22	165.60
	Summer	135.39	119.69	107.16	101.66	101.02	90.30	60.61
	Annual	825.06	803.47	796.26	792.53	774.36	761.73	697.38
Maximum temperature (°C)	Autumn	21.40	22.67	23.47	24.19	23.15	24.43	25.81
	Winter	11.06	12.15	12.91	13.45	12.42	13.86	14.72
	Spring	18.85	19.87	20.38	21.07	20.02	21.40	22.68
	Summer	29.40	30.72	31.48	32.34	31.13	32.76	34.27
	Annual	20.22	21.39	22.10	22.81	21.72	23.16	24.41
Minimum temperature (°C)	Autumn	12.74	13.91	14.77	15.44	14.30	15.57	16.87
	Winter	4.41	5.45	6.13	6.71	5.69	7.04	7.86
	Spring	9.39	10.38	10.83	11.53	10.35	11.65	12.77
	Summer	18.88	20.18	20.95	21.68	20.23	21.82	23.20
	Annual	11.38	12.51	13.20	13.87	12.67	14.05	15.21
Streamflow rate (m^3/s)	Autumn	0.25	0.24	0.23	0.21	0.19	0.17	0.10
	Winter	1.08	1.02	1.00	1.00	0.97	0.93	0.84
	Spring	0.50	0.49	0.51	0.48	0.48	0.49	0.40
	Summer	0.17	0.16	0.16	0.16	0.16	0.15	0.14
	Annual	0.50	0.48	0.47	0.46	0.45	0.43	0.37
Total net lake evaporation rate (mm)	Autumn	31.34	33.56	52.19	48.78	47.17	61.03	81.91
	Winter	0.00	0.00	0.00	0.00	0.00	0.00	0.00
	Spring	19.72	30.46	35.40	32.61	26.78	41.30	60.97
	Summer	152.81	190.25	215.58	234.57	212.72	250.74	305.49
	Annual	203.88	254.27	303.17	315.96	286.67	353.07	448.37
Total net irrigation requirement (hm^3)	Autumn	0.32	0.32	0.43	0.40	0.40	0.48	0.58
	Winter	0.00	0.00	0.00	0.00	0.00	0.00	0.00
	Spring	0.58	0.67	0.70	0.66	0.64	0.72	0.84
	Summer	2.94	3.25	3.47	3.62	3.46	3.78	4.26
	Annual	3.84	4.24	4.60	4.67	4.51	4.99	5.69

surface water and groundwater interaction in the Akmese Basin.

4.3 Analysis of changing climate impacts on irrigation demands and water availability

The mean annual ET_o and ET_c amounts of the Akmese irrigation site under the climate conditions of the CMIP6 historical experiment are estimated, in turn, to be 976.05 and 4974.80 mm for the 1990–2014 period. The estimated mean monthly ET_o and crop-based ET_c amounts are consistent with the reported values in TAGEM and DSI (2017). The projected increases in the mean annual ET_o amount are determined as 3.52, 5.55, and 7.73% under the SSP245 scenario and as 4.33, 8.68, and 12.66% under the SSP585 scenario, respectively, for the near-, mid-, and long-future periods. The ET_o increases lead to the corresponding rises in the mean annual total ET_c amount of the irrigated crops by 3.79, 5.73, and 7.87% under the SSP245 scenario and by 4.37, 8.92, and 12.84% under the SSP585 scenario, respectively, in the near-, mid-, and long-future periods. The seasonal and annual means of the net irrigation requirements of the Akmese irrigation scheme calculated by the CROPWAT model under the considered climate scenarios are provided in Table 7. Accordingly, while the mean annual total net irrigation demand in the baseline historical period of 1990–2014 is 3.84 hm^3, this amount increases in the near-, mid-, and long-future periods, in turn, by 10.30, 19.76, and

21.70% under the SSP245 scenario and by 17.43, 29.86, and 48.04% under the SSP585 emission scenario.

Considering the strong correlation between the long-term mean monthly total evaporation and temperature records of the Kocaeli MS with the coefficient of determination (r^2) of 0.88, the mean monthly net lake evaporation rates per unit area are calculated using the precipitation and temperature predictions of the CMIP6 Historical, CMIP6 SSP245, and CMIP6 SSP585, as summarized seasonally and annually in Table 7. Accordingly, while the annual net evaporation rate of the Akmese reservoir is computed as 203.88 mm for the baseline historical period of 1990–2014, this rate increases in the near-, mid-, and long-future periods, in turn, by 24.72, 48.70, and 54.98% under the SSP245 scenario and by 40.61, 73.18, and 119.92% under the SSP585 scenario. The monthly mean evaporated water amounts from the Akmese reservoir are calculated by multiplying the estimated mean monthly net evaporation rates with the actual mean reservoir area determined for each month of the 25-year reservoir operation considering the initial and ending reservoir storage areas.

The results of the 25-year reservoir operations conducted for the historical and three future periods with the changing inputs of monthly inflow rates, mean monthly net irrigation water demands, and mean monthly lake evaporation rates are summarized in Table 8. The conducted reservoir operation under the climate conditions of the CMIP6 historical experiment shows that the reservoir storage of the Akmese Dam is sufficient to supply all the domestic, environmental, and irrigation water demands at each month of the 25-year historical operation period of 1990–2014. According to the results of the reservoir operations conducted for the future periods, it is seen that the projected increases in the lake evaporation rates for the coming periods have a limited effect on the future lake evaporation amounts due to the decreases in the average reservoir levels. However, the projected increases in the irrigation water requirements and decreases in the inflow rates through the future periods result in considerable deficiencies in supplying the water demands, especially under the SSP585 scenario.

As detailed in Table 8, under the SSP245 emission scenario, the water supply problem is valid for only 3 months of the mid-future period, and the number of months with water deficit increases to 11 over the long-future period. In these periods, 0.59 and 1.86% of the total water demand cannot be met, respectively. Although significant decreases

Table 8 Operation results of the Akmese reservoir under historical and future climate conditions

Climate data			CMIP6 Historical	CMIP6 SSP245			CMIP6 SSP585		
Operation period			1990–2014	2025–2049	2050–2074	2075–2099	2025–2049	2050–2074	2075–2099
Inflow		m^3/s	0.50	0.48	0.47	0.46	0.45	0.43	0.37
		hm^3/year	15.79	15.05	14.88	14.51	14.20	13.62	11.65
Lake evaporation		hm^3/year	0.20	0.23	0.23	0.23	0.19	0.18	0.17
Spillway release		month	63	31	12	8	3	4	3
		m^3/s	0.29	0.25	0.37	0.35	0.78	0.74	0.56
		hm^3/year	1.92	0.81	0.46	0.29	0.24	0.30	0.17
Regulation		%	69.84	75.89	78.75	80.41	80.75	81.18	82.07
Water demand	Domestic	hm^3/year	7.19	7.19	7.19	7.19	7.19	7.19	7.19
	Environmental	hm^3/year	2.82	2.82	2.82	2.82	2.82	2.82	2.82
	Irrigation	hm^3/year	3.84	4.24	4.60	4.67	4.51	4.99	5.69
	Total	hm^3/year	13.85	14.25	14.61	14.69	14.52	15.00	15.70
Water supply	Domestic	hm^3/year	7.19	7.19	7.15	7.10	7.09	6.72	5.89
		%	100.00	100.00	99.56	98.79	98.67	93.84	83.39
	Environmental	hm^3/year	2.82	2.82	2.81	2.77	2.74	2.59	2.29
		%	100.00	100.00	99.33	97.49	95.56	88.20	73.59
	Irrigation	hm^3/year	3.84	4.24	4.56	4.57	4.38	4.34	3.68
		%	100.00	100.00	98.92	95.68	92.67	79.83	61.11
	Total	hm^3/year	13.85	14.25	14.53	14.44	14.20	13.65	11.86
		%	100.00	100.00	99.41	98.14	97.57	90.74	77.89
Water deficiency	Domestic	month	0	0	2	6	9	32	75
	Environmental	month	0	0	2	9	16	39	83
	Irrigation	month	0	0	3	11	17	50	97
	Total	month	0	0	3	11	17	50	99
		hm^3/year	0.00	0.00	0.08	0.24	0.32	1.35	3.84

are observed in the number and amount of spillway releases, the water deficiency problem is much more pronounced for the SSP585 scenario. Under the SSP585 emission scenario, even though the calculated flow regulation rates are above 80% for all three future periods, the reservoir storage capacity of the Akmese Dam becomes insufficient to meet the total water requirement in 17, 50, and 99 months over the near-, mid-, and long-future periods, respectively. The water deficit rates for the future periods are computed, in turn, to be 2.43, 9.26, and 22.11%. Since the water supply priority is given to domestic and environmental requirements in the operation algorithm, the deficiencies in the irrigation water supply are much higher than these rates. In the 2050–2074 and 2075–2099 periods, 20.17 and 38.89% of the total irrigation water demand cannot be supplied, respectively. The projected decreases in the volume of spillway releases for the future periods indicate that increasing the planned storage capacity of the Akmese reservoir may not be a remedy to mitigate the effects of climate change on water availability. Nevertheless, an optimal crop pattern selection could help alleviate the potential future water stress conditions (Dariane et al. 2021; Georgiou and Papamichail 2008; Homayounfar et al. 2014).

4.4 Limits and strengths of the study

A minimum of 25 years of flow data is required for reliable reservoir operation analyses and for the calibration and validation of SWAT models. The current hydrometric network of Turkey is not sufficient in terms of both quality and quantity (Altinbilek and Hatipoglu 2020). Most of the SGSs with continuous flow records of 25 years or more are located on the main river branches, while the SGSs on small tributaries mostly have relatively short and interrupted flow measurements. Additionally, the climatic variables required for hydrological modeling using SWAT include precipitation, maximum and minimum temperatures, wind speed, relative humidity, and solar radiation. Turkey's MS network consists mainly of stations located in provincial and district centers. However, many of the MSs in the district centers do not measure wind speed, relative humidity, and solar radiation. Moreover, their observation periods are relatively short and interrupted. Turkey has hundreds of irrigation dams that rely on relatively small basins for water supply. Most of these dams have been planned under limited historical streamflow and meteorological data conditions. Unfortunately, the planning studies for new dams continue to overlook the potential impacts of climate change, as is the case with the Akmese Project.

Although this insufficient station network situation forces the use of only the weather datasets from the Kocaeli MS in setting up the SWAT model and the use of flow records from the SGSs located in neighboring basins to extend the flow

records of the Akmese SGS for the calibration and verification of the SWAT model, remarkably, successful streamflow simulation results are achieved for both the calibration and verification stages of the model. Moreover, the agreement between the streamflow rates simulated under the climate conditions of the CMIP6 historical experiment and the historical inflow rates of the reservoir, calculated based on the extended streamflow records of the Akmese SGS, indicates that the use of a single MS does not pose issues in the reservoir inflow projections. Regarding the irrigation demands within the Akmese Project, the agreement of the ET_o and crop-based ET_c amounts estimated under the climate conditions of the CMIP6 historical experiment with the reported values in TAGEM and DSI (2017) confirms that the climate of the Akmese irrigation area can be represented by the Kocaeli MS. Furthermore, the high consistency between the projected precipitation and temperature anomalies for the coordinates of the Kocaeli MS and the regional anomalies projected by Bağçaci et al. (2021) for both the SSP245 and SSP585 scenarios increases the reliability of the streamflow and irrigation water requirement projections and, hence, the reservoir operation results attained for the future periods within the scope of the study.

5 Summary and conclusions

This study assesses whether a multi-purpose dam designed based on historical hydro-climatological data can provide a stable water supply in the face of potential changes in climate conditions, using the case of the Akmese Dam and Irrigation Project. The major outcomes of this assessment on the resilience of the Akmese Project to future climate change can be summarized as follows:

– The mean annual maximum and minimum temperature rates are projected to increase gradually through the future periods by up to 2.59 °C and 2.49 °C under the SSP245 scenario and 4.20 °C and 3.82 °C under the SSP585 scenario, respectively.

– The mean annual total precipitation is projected to decrease gradually up to 3.94% in the long-future period under the SSP245 scenario, and under the SSP585 scenario, the decrease is anticipated to be more significant with the projected reductions of 6.14, 7.68, and 15.47% in the near-, mid-, and long-future periods, respectively.

– The summer precipitation declines are much more pronounced than the annual declines for both emission scenarios.

– A gradual decrease reaching up to 8.05% in the long-future period is projected for the mean annual inflow rates of the future periods under the SSP245 scenario, while the annual inflow reductions in the near-, mid, and

long-future periods under the SSP585 scenario are estimated, in turn, to be 10.00, 13.59, and 26.17%.

– The declines in the autumn inflows are significantly greater than the annual inflow decreases for both emission scenarios, primarily due to the considerably lower rainfall concentrations in the summer seasons.

– The mean annual total irrigation requirement is projected to gradually increase through future periods by up to 21.70 and 48.04% under the SSP245 and SSP585 scenarios, respectively.

– Despite the projected significant increases in the lake evaporation rates for the future periods, the estimated lake evaporation amounts for both emission scenarios are comparable to those observed in the historical period.

– The estimated water deficits in the three future periods under the SSP585 scenario are significantly higher than those under the SSP245 scenario.

– In the case of the SSP585 scenario, the projected hydro-climatic changes in the Akmese Basin may lead to the inability to meet 9.26 and 22.11% of the total water demand, as well as 20.17 and 38.89% of the total irrigation requirement in the mid- and long-future periods, respectively.

The unmet water demands demonstrate the need for planning and management strategies developed by considering the hydrological implications of future climate change (El-Nashar and Elyamany 2022; Haro-Monteagudo et al. 2022). These strategies are necessary to provide long-term sustainability of dam projects and, consequently, agricultural activities in basins such as Akmese, where water is typically scarce and is foreseen to become even scarcer under a warming and drying climate. Determining an optimal cropping pattern and developing water allocation and reservoir release policies accordingly seem to be a viable solution to overcome the potential impacts of future climate change on the water balance of the Akmese reservoir. The proposed framework can be further enhanced by considering future changes in the other climatic variables (i.e., solar radiation, wind speed, and relative humidity) in simulating inflow projections and in applying the FAO Penman–Monteith method (Gorguner and Kavvas 2020). In addition, further research experimenting with different bias correction techniques and averaging approaches in generating multi-model ensemble means is recommended to enhance the accuracy of precipitation predictions (Kim et al. 2016). In conclusion, the findings of this research should be interpreted as demonstrating the sensitivity of water storage and reservoir outflows to future precipitation and temperature projections under the SSP245 and SSP585 climate scenarios of CMIP6 for the Mediterranean basins. Considering the projected water supply risks for the Akmese Project, it is recommended that the water resource projects designed and managed based on only historical hydro-meteorological data should be reexamined for climate change adaptation and mitigation options by considering potential future climatic conditions through their operational lifetimes.

Author contribution EY: conceptualization, methodology, writing–review and editing.

Data availability Data will be made available on reasonable request.

Code availability Code will be made available on reasonable request.

Declarations

Competing interests The authors declare no competing interests.

Ethics approval Not applicable.

Consent to participate Not applicable.

Consent for publication Not applicable.

References

Abbaspour KC (2015) SWAT-CUP2: SWAT calibration and uncertainty programs - a user manual. Eawag - Swiss Federal Institute of Aquatic Science and Technology, Duebendorf

Abbaspour KC, Johnson CA, van Genuchten MT (2004) Estimating uncertain flow and transport parameters using a sequential uncertainty fitting procedure. Vadose Zone J 3(4):1340–1352. https://doi.org/10.2136/vzj2004.1340

Abbaspour KC, Yang J, Maximov I, Siber R, Bogner K, Mieleitner J, Zobrist J, Srinivasan R (2007) Modelling hydrology and water quality in the pre-alpine/alpine Thur watershed using SWAT. J Hydrol 333(2–4):413–430. https://doi.org/10.1016/j.jhydrol.2006.09.014

Abbaspour KC, Rouholahnejad E, Vaghefi S, Srinivasan R, Yang H, Kløve B (2015) A continental-scale hydrology and water quality model for Europe: calibration and uncertainty of a high-resolution large-scale SWAT model. J Hydrol 524:733–752. https://doi.org/10.1016/j.jhydrol.2015.03.027

Ahmed K, Sachindra DA, Shahid S, Demirel MC, Chung E-S (2019) Selection of multi-model ensemble of general circulation models for the simulation of precipitation and maximum and minimum temperature based on spatial assessment metrics. Hydrol Earth Syst Sci 23(11):4803–4824. https://doi.org/10.5194/hess-23-4803-2019

Ali E, Cramer W, Carnicer J, Georgopoulou E, Hilmi NJM, Le Cozannet G, Lionello P (2022) Cross-chapter paper 4: Mediterranean region. In: Pörtner H-O, Roberts DC, Tignor M, Poloczanska ES, Mintenbeck K, Alegría A, Craig M, Langsdorf S, Löschke S, Möller V, Okem A, Rama B (eds) Climate change 2022: impacts, adaptation and vulnerability (contribution of working group II to the sixth assessment report of the Intergovernmental Panel on Climate Change). Cambridge University Press, Cambridge and New York, pp 2233–2272

Allen RG, Pereira LS, Raes D, Smith M (1998) Crop evapotranspiration: guidelines for computing crop water requirements (FAO irrigation and drainage paper no:56). Food and Agricultural Organization of the United Nations, Rome

Almeida MP, Perpiñán O, Narvarte L (2015) PV power forecast using a nonparametric PV model. Sol Energy 115:354–368. https://doi.org/10.1016/j.solener.2015.03.006

Altinbilek D, Hatipoglu MA (2020) Water resources development. In: Harmancioglu NB, Altinbilek D (eds) Water resources of Turkey. Springer, Cham, pp 61–84

Ansley RJ, Boutton TW, Jacoby PW (2014) Root biomass and distribution patterns in a semi-arid mesquite savanna: responses to long-term rainfall manipulation. Rangeland Ecol Manage 67(2):206–218. https://doi.org/10.2111/REM-D-13-00119.1

Arnold JG, Kiniry JR, Srinivasan R, Williams JR, Haney EB, Neitsch SL (2013) SWAT 2012 input/output documentation. Texas Water Resources Institute, Texas

Bağçaci SÇ, Yucel I, Duzenli E, Yilmaz MT (2021) Intercomparison of the expected change in the temperature and the precipitation retrieved from CMIP6 and CMIP5 climate projections: a Mediterranean hot spot case. Turkey. Atmos Res 256:105576. https://doi.org/10.1016/j.atmosres.2021.105576

Bolle H-J (2003) Mediterranean climate: variability and trends. Springer-Verlag, Berlin and Heidelberg

Braca G, Bussettini M, Ducci D, Lastoria B, Mariani S (2019) Evaluation of national and regional groundwater resources under climate change scenarios using a GIS-based water budget procedure. Rend Fis Acc Lincei 30:109–123. https://doi.org/10.1007/s12210-018-00757-6

Chen W, Jiang Z, Li L (2011) Probabilistic projections of climate change over China under the SRES A1B scenario using 28 AOGCMs. J Climate 24(17):4741–4756. https://doi.org/10.1175/2011JCLI4102.1

Cherif S, Doblas-Miranda E, Lionello P, Borrego C, Giorgi F, Iglesias A, Jebari S, Mahmoudi E, Moriondo M, Pringault O, Rilov G, Somot S, Tsikliras A, Vila M, Zittis G (2020) Drivers of change. In: Cramer W, Guiot J, Marini K (eds) Climate and environmental change in the Mediterranean Basin - current situation and risks for the future (first Mediterranean assessment report). Union for the Mediterranean, Plan Bleu, UNEP/MAP, Marseille, pp 59–180

Choukr-Allah R, Ragab R, Rodríguez-Clemente R (2012) Integrated water resources management in the Mediterranean region: dialogue towards new strategy. Springer, Dordrecht

Correia FN (1999) Water resources in the Mediterranean region. Water Int 24(1):22–30. https://doi.org/10.1080/02508069908692130

Cos J, Doblas-Reyes F, Jury M, Marcos R, Bretonnière P-A, Samsó M (2022) The Mediterranean climate change hotspot in the CMIP5 and CMIP6 projections. Earth Syst Dynam 13(1):321–340. https://doi.org/10.5194/esd-13-321-2022

Cudennec C, Leduc C, Koutsoyiannis D (2007) Dryland hydrology in Mediterranean regions - a review. Hydrol Sci J 52(6):1077–1087. https://doi.org/10.1623/hysj.52.6.1077

Cygwin (2022) Cygwin user's guide. https://www.cygwin.com/cygwin-ug-net/cygwin-ug-net.pdf. Accessed 20 May 2022

Daccache A, Ciurana JS, Rodriguez Diaz JA, Knox JW (2014) Water and energy footprint of irrigated agriculture in the Mediterranean region. Environ Res Lett 9(12):124014. https://doi.org/10.1088/1748-9326/9/12/124014

Dariane AB, Ghasemi M, Karami F, Azaranfar A, Hatami S (2021) Crop pattern optimization in a multi-reservoir system by combining many-objective and social choice methods. Agr Water Manage 257:107162. https://doi.org/10.1016/j.agwat.2021.107162

DSI General Directorate of State Hydraulic Works (2022) Flow gauging yearbooks (1959–2015). General Directorate of State Hydraulic Works, Ankara

EC-JRC (European Commission - Joint Research Centre) (2006) The Global Land Cover 2000 (GLC2000) products. https://forobs.jrc.ec.europa.eu/products/glc2000/products.php. Accessed 28 June 2022

El-Nashar W, Elyamany A (2022) Adapting irrigation strategies to mitigate climate change impacts: a value engineering approach. Water Resour Manage 1–18. https://doi.org/10.1007/s11269-022-03353-4

ESGF (Earth System Grid Federation) (2022) WCRP Coupled Model Intercomparison Project (phase 6). https://esgf-node.llnl.gov/projects/cmip6/. Accessed 15 May 2022

Eyring V, Bony S, Meehl GA, Senior CA, Stevens B, Stouffer RJ, Taylor KE (2016) Overview of the Coupled Model Intercomparison Project Phase 6 (CMIP6) experimental design and organization. Geosci Model Dev 9(5):1937–1958. https://doi.org/10.5194/gmd-9-1937-2016

FAO (Food and Agriculture Organization of the United Nations) (2007) Digital Soil Map of the World (DSMW). https://www.fao.org/geonetwork/srv/en/metadata.show?id=14116. Accessed 28 June 2022

Forster PM, Maycock AC, McKenna CM, Smith CJ (2020) Latest climate models confirm need for urgent mitigation. Nat Clim Change 10:7–10. https://doi.org/10.1038/s41558-019-0660-0

Georgiou PE, Papamichail DM (2008) Optimization model of an irrigation reservoir for water allocation and crop planning under various weather conditions. Irrig Sci 26:487–504. https://doi.org/10.1007/s00271-008-0110-7

Giorgi F (2006) Climate change hot-spots. Geophys Res Lett 33(8):L08707. https://doi.org/10.1029/2006GL025734

Gorguner M, Kavvas ML (2020) Modeling impacts of future climate change on reservoir storages and irrigation water demands in a Mediterranean basin. Sci Total Environ 748:141246. https://doi.org/10.1016/j.scitotenv.2020.141246

Gupta HV, Kling H, Yilmaz KK, Martinez GF (2009) Decomposition of the mean squared error and NSE performance criteria: implications for improving hydrological modelling. J Hydrol 377(1–2):80–91. https://doi.org/10.1016/j.jhydrol.2009.08.003

Haro-Monteagudo D, Palazón L, Beguería S (2020) Long-term sustainability of large water resource systems under climate change: a cascade modeling approach. J Hydrol 582:124546. https://doi.org/10.1016/j.jhydrol.2020.124546

Haro-Monteagudo D, Palazón L, Zoumides C, Beguería S (2022) Optimal implementation of climate change adaptation measures to ensure long-term sustainability on large irrigation systems. Water Resour Manage 1–16. https://doi.org/10.1007/s11269-022-03225-x

Hoegh-Guldberg O, Jacob D, Taylor M, Bindi M, Brown S, Camilloni I, Diedhiou A, Djalante R, Ebi KL, Engelbrecht F, Guiot J, Hijioka Y, Mehrotra S, Payne A, Seneviratne SI, Thomas A, Warren R, Zhou G (2022) Impacts of 1.5°C global warming on natural and human systems. In: Masson-Delmotte V, Zhai P, Pörtner H-O, Roberts D, Skea J, Shukla PR, Pirani A, Moufouma-Okia W, Péan C, Pidcock R, Connors S, Matthews JBR, Chen Y, Zhou X, Gomis MI, Lonnoy E, Maycock T, Tignor M, Waterfield T (eds) Global warming of 1.5°C (An IPCC special report on the impacts of global warming of 1.5°C above pre-industrial levels and related global greenhouse gas emission pathways, in the context of strengthening the global response to the threat of climate change, sustainable development, and efforts to eradicate poverty). Cambridge University Press, Cambridge and New York, 175–312

Homayounfar M, Lai SH, Zomorodian M, Sepaskhah AR, Ganji A (2014) Optimal crop water allocation in case of drought occurrence, imposing deficit irrigation with proportional cutback constraint. Water Resour Manage 28:3207–3225. https://doi.org/10.1007/s11269-014-0669-0

Iglesias A, Garrote L, Flores F, Moneo M (2007) Challenges to manage the risk of water scarcity and climate change in the Mediterranean. Water Resour Manage 21:775–788. https://doi.org/10.1007/s11269-006-9111-6

Iturbide M, Gutiérrez JM, Alves LM, Bedia J, Cerezo-Mota R, Cimadevilla E, Cofiño AS, Di Luca A, Faria SH, Gorodetskaya

IV, Hauser M, Herrera S, Hennessy K, Hewitt HT, Jones RG, Krakovska S, Manzanas R, Martínez-Castro D, Narisma GT, Nurhati IS, Pinto I, Seneviratne SI, van den Hurk B, Vera CS (2020) An update of IPCC climate reference regions for subcontinental analysis of climate model data: definition and aggregated datasets. Earth Syst Sci Data 12(4):2959–2970. https://doi.org/10.5194/essd-12-2959-2020

Jiménez Cisneros BE, Oki T, Arnell NW, Benito G, Cogley JG, Döll P, Jiang T, Mwakalila SS (2014) Freshwater resources. In: Field CB, Barros VR, Dokken DJ, Mach KJ, Mastrandrea MD, Bilir TE, Chatterjee M, Ebi KL, Estrada YO, Genova RC, Girma B, Kissel ES, Levy AN, MacCracken S, Mastrandrea PR, White LL (eds) Climate change 2014: impacts, adaptation, and vulnerability - part b: global and sectoral aspects (contribution of working group II to the fifth assessment report of the Intergovernmental Panel on Climate Change). Cambridge University Press, Cambridge and New York, pp 229–269

Jones PW (1999) First- and second-order conservative remapping schemes for grids in spherical coordinates. Mon Weather Rev 127(9):2204–2210. https://doi.org/10.1175/1520-0493(1999)127%3c2204:FASOCR%3e2.0.CO;2

Kim J, Ivanov VY, Fatichi S (2016) Climate change and uncertainty assessment over a hydroclimatic transect of Michigan. Stoch Environ Res Risk Assess 30:923–944. https://doi.org/10.1007/s00477-015-1097-2

Knutti R, Sedláček J (2013) Robustness and uncertainties in the new CMIP5 climate model projections. Nat Clim Change 3:369–373. https://doi.org/10.1038/nclimate1716

Kondolf GM, Batalla RJ (2005) Hydrological effects of dams and water diversions on rivers of Mediterranean-climate regions: examples from California. In: Garcia C, Ramon J, Batalla RJ (eds) Catchment dynamics and river processes: Mediterranean and other climate region (Developments in Earth Surface Processes, vol.7). Elsevier, 197–211. https://doi.org/10.1016/S0928-2025(05)80017-3

Koutroulis AG, Grillakis MG, Daliakopoulos IN, Tsanis IK, Jacob D (2016) Cross sectoral impacts on water availability at +2°C and +3°C for east Mediterranean island states: the case of Crete. J Hydrol 532:16–28. https://doi.org/10.1016/j.jhydrol.2015.11.015

Kovats RS, Valentini R, Bouwer LM, Georgopoulou E, Jacob D, Martin E, Rounsevell M, Soussana J-F (2014) Europe. In: Barros VR, Field CB, Dokken DJ, Mastrandrea MD, Mach KJ, Bilir TE, Chatterjee M, Ebi KL, Estrada YO, Genova RC, Girma B, Kissel ES, Levy AN, MacCracken S, Mastrandrea PR, White LL (eds) Climate change 2014: impacts, adaptation, and vulnerability - part b: regional aspects (contribution of working group II to the fifth assessment report of the Intergovernmental Panel on Climate Change). Cambridge University Press, Cambridge and New York, pp 1267–1326

Kumar D, Kodra E, Ganguly AR (2014) Regional and seasonal intercomparison of CMIP3 and CMIP5 climate model ensembles for temperature and precipitation. Clim Dyn 43:2491–2518. https://doi.org/10.1007/s00382-014-2070-3

Legates DR, McCabe GJ (1999) Evaluating the use of "goodness-of-fit" measures in hydrologic and hydroclimatic model validation. Water Resour Res 35(1):233–241. https://doi.org/10.1029/1998WR900018

Lionello P, Malanotte-Rizzoli P, Boscolo R, Alpert P, Artale V, Li L, Luterbacher J, May W, Trigo R, Tsimplis M, Ulbrich U, Xoplaki E (2006) The Mediterranean climate: an overview of the main characteristics and issues. In: Lionello P, Malanotte-Rizzoli P, Boscolo R (eds) Mediterranean climate variability (Developments in Earth and Environmental Sciences, vol.4). Elsevier, 1–26. https://doi.org/10.1016/S1571-9197(06)80003-0

López-Moreno JI, Zabalza J, Vicente-Serrano SM, Revuelto J, Gilaberte M, Azorin-Molina C, Morán-Tejeda E, García-Ruiz JM,

Tague C (2014) Impact of climate and land use change on water availability and reservoir management: scenarios in the upper Aragón River, Spanish Pyrenees. Sci Total Environ 493:1222–1231. https://doi.org/10.1016/j.scitotenv.2013.09.031

Masia S, Sušnik J, Marras S, Mereu S, Spano D, Trabucco A (2018) Assessment of irrigated agriculture vulnerability under climate change in Southern Italy. Water 10(2):209. https://doi.org/10.3390/w10020209

MGM (Turkish State Meteorological Service) (2022a) Daily precipitation, maximum and minimum air temperature, solar radiation, wind speed, and relative humidity records of the Kocaeli meteorological station (station ID: 17066). Turkish State Meteorological Service, Ankara

MGM (Turkish State Meteorological Service) (2022b) Long-term all parameters bulletin for the Akmese meteorological station (station IDs: 1532 and 18799). Turkish State Meteorological Service, Ankara

MGM (Turkish State Meteorological Service) (2022c) Long-term all parameters bulletin for the Kocaeli meteorological station (station ID: 17066). Turkish State Meteorological Service, Ankara

Michaelides S, Karacostas T, Sánchez JL, Retalis A, Pytharoulis I, Homar V, Romero R, Zanis P, Giannakopoulos C, Bühl J, Ansmann A, Merino A, Melcón P, Lagouvardos K, Kotroni V, Bruggeman A, López-Moreno JI, Berthet C, Katragkou E, Tymvios F, Hadjimitsis DG, Mamouri R-E, Nisantzi A (2018) Reviews and perspectives of high impact atmospheric processes in the Mediterranean. Atmos Res 208:4–44. https://doi.org/10.1016/j.atmosres.2017.11.022

Milano M, Ruelland D, Fernandez S, Dezetter A, Fabre J, Servat E, Fritsch J-M, Ardoin-Bardin S, Thivet G (2013) Current state of Mediterranean water resources and future trends under climatic and anthropogenic changes. Hydrol Sci J 58(3):498–518. https://doi.org/10.1080/02626667.2013.774458

Montaldo N, Oren R (2018) Changing seasonal rainfall distribution with climate directs contrasting impacts at evapotranspiration and water yield in the Western Mediterranean region. Earth's Future 6(6):841–856. https://doi.org/10.1029/2018EF000843

Moriasi DN, Arnold JG, Van Liew MW, Bingner RL, Harmel RD, Veith TL (2007) Model evaluation guidelines for systematic quantification of accuracy in watershed simulations. T Asabe 50(3):885–900. https://doi.org/10.13031/2013.23153

Mrabet R, Savé R, Toreti A, Caiola N, Chentouf M, Llsat MC, Mohamed AAA, Santeramo FG, Sanz-Cobena A, Tskliras A (2020) Food. In: Cramer W, Guiot J, Marini K (eds) Climate and environmental change in the Mediterranean Basin - current situation and risks for the future (first Mediterranean assessment report). Union for the Mediterranean, Plan Bleu, UNEP/MAP, Marseille, pp 237–264

Nash JE, Sutcliffe JV (1970) River flow forecasting through conceptual models part I - a discussion of principles. J Hydrol 10(3):282–290. https://doi.org/10.1016/0022-1694(70)90255-6

Neitsch SL, Arnold JG, Kiniry JR, Williams JR (2011) Soil and Water Assessment Tool theoretical documentation version 2009. Texas Water Resources Institute, Texas

Nunes JP, Jacinto R, Keizer JJ (2017) Combined impacts of climate and socio-economic scenarios on irrigation water availability for a dry Mediterranean reservoir. Sci Total Environ 584–585:219–233. https://doi.org/10.1016/j.scitotenv.2017.01.131

O'Neill BC, Tebaldi C, van Vuuren DP, Eyring V, Friedlingstein P, Hurtt G, Knutti R, Kriegler E, Lamarque J-F, Lowe J, Meehl GA, Moss R, Riahi K, Sanderson BM (2016) The Scenario Model Intercomparison Project (ScenarioMIP) for CMIP6. Geosci Model Dev 9(9):3461–3482. https://doi.org/10.5194/gmd-9-3461-2016

Okkan U, Kirdemir U (2018) Investigation of the behavior of an agricultural-operated dam reservoir under RCP scenarios of AR5-IPCC. Water Resour Manage 32:2847–2866. https://doi.org/10.1007/s11269-018-1962-0

Rathjens H, Bieger K, Srinivasan R, Chaubey I, Arnold JG (2016) CMhyd user manual: documentation for preparing simulated climate change data for hydrologic impact studies. https://swat.tamu.edu/media/115265/bias_cor_man.pdf. Accessed 25 May 2022

Roberts NM, Lean HW (2008) Scale-selective verification of rainfall accumulations from high-resolution forecasts of convective events. Mon Weather Rev 136(1):78–97. https://doi.org/10.1175/2007MWR2123.1

Rocha J, Carvalho-Santos C, Diogo P, Beça P, Keizer JJ, Nunes JP (2020) Impacts of climate change on reservoir water availability, quality and irrigation needs in a water scarce Mediterranean region (southern Portugal). Sci Total Environ 736:139477. https://doi.org/10.1016/j.scitotenv.2020.139477

Schulzweida U (2021) CDO user guide version 2.0.5. Max Planck Institute for Meteorology, Hamburg

Seker M, Gumus V (2022) Projection of temperature and precipitation in the Mediterranean region through multi-model ensemble from CMIP6. Atmos Res 280:106440. https://doi.org/10.1016/j.atmosres.2022.106440

Şen Z (2015) Applied drought modeling, prediction, and mitigation. Elsevier, Amsterdam

Siqueira PP, Oliveira PTS, Bressiani D, Neto AAM, Rodrigues DB (2021) Effects of climate and land cover changes on water availability in a Brazilian Cerrado basin. J Hydrol Reg Stud 37:100931. https://doi.org/10.1016/j.ejrh.2021.100931

Smith M (1992) CROPWAT - a computer program for irrigation planning and management (FAO irrigation and drainage paper no:46). Food and Agricultural Organization of the United Nations, Rome

Stocker TF, Qin D, Plattner G-K, Alexander LV, Allen SK, Bindoff NL, Bréon F-M, Church JA, Cubasch U, Emori S, Forster P, Friedlingstein P, Gillett N, Gregory JM, Hartmann DL, Jansen E, Kirtman B, Knutti R, Krishna Kumar K, Lemke P, Marotzke J, Masson-Delmotte V, Meehl GA, Mokhov II, Piao S, Ramaswamy V, Randall D, Rhein M, Rojas M, Sabine C, Shindell D, Talley LD, Vaughan DG, Xie S-P (2013) Technical summary. In: Stocker TF, Qin D, Plattner G-K, Tignor M, Allen SK, Boschung J, Nauels A, Xia Y, Bex V, Midgley PM (eds) Climate change 2013: the physical science basis (contribution of working group I to the fifth assessment report of the Intergovernmental Panel on Climate Change). Cambridge University Press, Cambridge and New York

Stouffer RJ, Eyring V, Meehl GA, Bony S, Senior C, Stevens B, Taylor KE (2017) CMIP5 scientific gaps and recommendations for CMIP6. Bull Am Meteorol Soc 98(1):95–105. https://doi.org/10.1175/BAMS-D-15-00013.1

Sun C, Zhu L, Liu Y, Wei T, Guo Z (2022) CMIP6 model simulation of concurrent continental warming holes in Eurasia and North America since 1990 and their relation to the Indo-Pacific SST warming. Global Planet Change 213:103824. https://doi.org/10.1016/j.gloplacha.2022.103824

TAGEM (General Directorate of Agricultural Research and Policies), DSI (General Directorate of State Hydraulic Works) (2017) Plant water consumption of irrigated plants in Turkey. General Directorate of Agricultural Research and Policies & General Directorate of State Hydraulic Works, Ankara

Temelsu (Temelsu International Engineering Services Incorporated Company) (2016a) The Kocaeli Akmese Dam and Irrigation Project planning report. Temelsu International Engineering Services Incorporated Company, Ankara

Temelsu (Temelsu International Engineering Services Incorporated Company) (2016b) The Kocaeli Akmese Dam and natural building material quarries project (including ready concrete and crushing-screening plants) environmental impact assessment application report. Temelsu International Engineering Services Incorporated Company, Ankara

Tramblay Y, Koutroulis A, Samaniego L, Vicente-Serrano SM, Volaire F, Boone A, Page ML, Llasat MC, Albergel C, Burak S, Cailleret M, Kalin KC, Davi H, Dupuy J-L, Greve P, Grillakis M, Hanich L, Jarlan L, Martin-StPaul N, Martínez-Vilalta J, Mouillot F, Pulido-Velazquez D, Quintana-Seguí P, Renard D, Turco M, Türkeş M, Trigo R, Vidal J-P, Vilagrosa A, Zribi M, Polcher J (2020) Challenges for drought assessment in the Mediterranean region under future climate scenarios. Earth-Sci Rev 210:103348. https://doi.org/10.1016/j.earscirev.2020.103348

UNDP (United Nations Development Programme) (2006) Human development report 2006 - beyond scarcity: power, poverty and the global water crisis. United Nations Development Programme, New York

USDA-SCS (United States Department of Agriculture, Soil Conservation Service) (1970) Irrigation water requirements (Technical release no:21). United States Department of Agriculture, Soil Conservation Service, Washington

USGS (United States Geological Survey) (2014) Shuttle Radar Topography Mission (SRTM): 1 arc-second global elevation database. https://earthexplorer.usgs.gov/. Accessed 28 June 2022

Usul N (2009) Engineering hydrology. METU Press, Ankara

Valverde P, Serralheiro R, de Carvalho M, Maia R, Oliveira B, Ramos V (2015) Climate change impacts on irrigated agriculture in the Guadiana river basin (Portugal). Agr Water Manage 152:17–30. https://doi.org/10.1016/j.agwat.2014.12.012

Wyser K, Kjellström E, Koenigk T, Martins H, Döscher R (2020) Warmer climate projections in EC-Earth3-Veg: the role of changes in the greenhouse gas concentrations from CMIP5 to CMIP6. Environ Res Lett 15(5):054020. https://doi.org/10.1088/1748-9326/ab81c2

Yalcin E (2019) Estimation of irrigation return flow on monthly time resolution using SWAT model under limited data availability. Hydrol Sci J 64(13):1588–1604. https://doi.org/10.1080/02626667.2019.1662025

Yang H, Zehnder AJB (2002) Water scarcity and food import: a case study for southern Mediterranean countries. World Dev 30(8):1413–1430. https://doi.org/10.1016/S0305-750X(02)00047-5

Zittis G, Almazroui M, Alpert P, Ciais P, Cramer W, Dahdal Y, Fnais M, Francis D, Hadjinicolaou P, Howari F, Jrrar A, Kaskaoutis DG, Kulmala M, Lazoglou G, Mihalopoulos N, Lin X, Rudich Y, Sciare J, Stenchikov G, Xoplaki E, Lelieveld J (2022) Climate change and weather extremes in the Eastern Mediterranean and Middle East. Rev Geophys 60(3):e2021RG000762. https://doi.org/10.1029/2021RG000762